

ORIGINAL RESEARCH ARTICLE



Circulating Extracellular Vesicles in the Pathogenesis of Heart Failure in Patients With Chronic Kidney Disease

Xisheng Li^{ID}, PhD*; Nikhil Raisinghani, MBBS*; Alex Gallinat^{ID}, PhD; Carlos G. Santos-Gallego^{ID}, MD; Shihong Zhang^{ID}, BS; Sabrina La Salvia, PhD; Seonghun Yoon^{ID}, PhD; Hayrettin Yavuz^{ID}, MD, PhD; Anh Phan^{ID}, PhD; Alan Shao, BS; Michael Harding, PhD; David Sachs^{ID}, PhD; Carol J. Levy^{ID}, MD; Navneet Dogra^{ID}, PhD; Rupangi Vasavada, PhD; Nicole C. Dubois, PhD; Uta Erdbrügger, MD; Susmita Sahoo^{ID}, PhD

BACKGROUND: Cardiovascular disease causes >50% of deaths in patients with advanced chronic kidney disease (CKD). Clinical studies suggest that kidney-derived factors contribute to cardiovascular disease development in CKD, independently of comorbidities. However, to date, no kidney-specific humoral risk factor that triggers direct cardiotoxicity has been identified. In this cross-sectional study, we investigate how, in patients with CKD, circulating extracellular vesicles (EVs) facilitate pathological kidney-heart communication, thereby causing cardiotoxicity, impairing cardiac function, and contributing to heart failure progression.

METHODS: We investigated the function of EVs from patients with CKD and adenine diet–induced CKD mice on cardiomyocyte and cardiac contractility. microRNA (miRNA) cargo of EVs was identified by small RNA sequencing and quantitative reverse transcription polymerase chain reaction, and their cardiotoxicity was tested by using miRNA mimics. Tissue and cellular origin of CKD-EV-miRNAs were determined from their corresponding primary miRNA expressions in mice.

RESULTS: EVs from plasma of patients with CKD, but not from healthy controls, were cardiotoxic; they significantly induced apoptosis both *in vitro* and *in vivo* and impaired contractility of adult rat primary cardiomyocytes *in vitro*. Likewise, EVs from both plasma and kidneys of CKD mice were cardiotoxic. Pharmacologically depleting circulating EVs in CKD mice significantly recovered cardiac function and ameliorated heart failure, improvements that suggest CKD-EVs play a causal role in heart failure pathogenesis. Both human and mouse CKD-EVs were enriched in distinct miRNAs compared with control EVs. CKD-EV-miRNA mimics were cardiotoxic, impairing contractility and downregulating contractile gene expression in human induced pluripotent stem cell–derived cardiomyocytes. It is interesting that levels of endogenous primary miRNAs corresponding to circulating CKD-EV-miRNAs were significantly higher in CKD kidney tissues, specifically in CD45^{-ve}CD31^{-ve} renal cells, but not in CKD hearts, CKD livers, or CKD-peripheral blood mononuclear cells, a result that indicates CKD-EV-miRNAs originate renally. It is remarkable that CKD-EV-miRNA levels correlated with established markers of cardiac injury, thus uncovering the presence of subclinical heart disease and demonstrating heterogeneity in reno-cardiac disease.

CONCLUSIONS: Collectively, our human subject and mouse studies show that circulating CKD-EVs, carrying distinct renal-derived miRNAs, mediate the molecular crosstalk that contributes to the pathogenesis of heart failure in CKD. Consequently, CKD-EVs hold promise as diagnostic and prognostic biomarkers for early disease detection and as targets for novel therapeutic interventions in chronic reno-cardiac disease.

Key Words: circulating microRNA ■ extracellular vesicles ■ heart failure ■ myocardial contraction ■ renal insufficiency, chronic

Correspondence to: Susmita Sahoo, PhD, Icahn School of Medicine at Mount Sinai, One Gustave L. Levy Pl, Box 1030, New York, NY 10029-6574. Email susmita.sahoo@mssm.edu

*X. Li and N. Raisinghani contributed equally.

This work was presented as an abstract at AHA Scientific Sessions, New Orleans, LA, November 7–10, 2025.

Supplemental Material is available at <https://www.ahajournals.org/doi/suppl/10.1161/CIRCULATIONAHA.125.075579>.

For Sources of Funding and Disclosures, see page 112.

© 2025 The Authors. *Circulation* is published on behalf of the American Heart Association, Inc., by Wolters Kluwer Health, Inc. This is an open access article under the terms of the [Creative Commons Attribution Non-Commercial-NoDerivs](#) License, which permits use, distribution, and reproduction in any medium, provided that the original work is properly cited, the use is noncommercial, and no modifications or adaptations are made.

Circulation is available at www.ahajournals.org/journal/circ

Clinical Perspective

What Is New?

- Using human, mouse, and cell culture models, we show that circulating chronic kidney disease (CKD) extracellular vesicles (EVs) are cardiotoxic; they induce apoptosis, impair contractility, and restrict calcium handling in treated cardiomyocytes.
- CKD-EVs carry distinct CKD-EV-microRNAs that are primarily of renal origin.
- This CKD-EV-mediated molecular crosstalk between the kidneys and the heart plays a causal role in the pathogenesis of heart failure in patients with CKD.

What Are the Clinical Implications?

- CKD-EV-microRNAs correlate with established markers of cardiac injury, thus uncovering the presence of subclinical heart disease and heterogeneity in patients with CKD not yet diagnosed with heart failure.
- Our work aids in defining the complex relationship between CKD and heart failure and the different disease phenotypes along the reno-cardiac axis.
- CKD-microRNAs are promising biomarkers for early disease detection and potential targets for novel therapeutic interventions in chronic reno-cardiac disease.

Nonstandard Abbreviations and Acronyms

CKD	chronic kidney disease
CM	cardiomyocyte
EV	extracellular vesicle
GW	GW4869
hAC16	human AC16
hCKD-EV	EV from patient with CKD
hCtr-EV	EV from healthy control
HF	heart failure
hiPSC	human induced pluripotent stem cell-derived
LV	left ventricle
mCKD-kEV	kidney EV from CKD mouse
mCKD-pEV	plasma EV from CKD mouse
mCtr-kEV	kidney EV from control mouse
mCtr-pEV	plasma EV from control mouse
miRNA	microRNA
NT-proBNP	N-terminal pro-B-type natriuretic peptide
pri-miRNA	primary miRNA

in >3 million deaths worldwide in 2019.¹ Although CKD is a direct cause of morbidity and mortality, it is also an important risk factor for cardiovascular disease (CVD).² Indeed, the degree of CVD correlates with CKD severity. In patients with early-stage CKD (stages 1 and 2), CVD incidence is significantly higher than in the general population.³ CVD mortality risk doubles and triples during CKD stages 3 and 4, respectively. Moreover, CVD is the leading cause of death during end-stage CKD (stage 5).^{3,4}

The relationship between heart failure (HF) and CKD is close and complex. A better understanding of HF pathophysiology is necessary to develop prevention and treatment strategies to reduce the high morbidity and mortality in patients with CKD. Traditional risk factors, such as hypertension, hyperlipidemia, smoking, and diabetes, are prevalent in patients with CKD; however, these comorbidities do not fully explain the elevated cardiovascular risk in patients with CKD.⁵ Pathophysiological dysfunctions associated with CKD can induce other nontraditional risk factors, such as inflammation, oxidative stress, and abnormal calcium-phosphorus metabolism, which may contribute to HF progression.² Nevertheless, kidney-specific humoral risk factors that cause early functional and structural cardiac damage have yet to be determined, largely because populations with reno-cardiac disease remain understudied. Thus, there is an urgent need to identify novel mediators of HF onset in patients with CKD.

Emerging evidence shows that circulating extracellular vesicles (EVs) facilitate long-distance cell-to-cell communication and mediate organ crosstalk.⁶ The molecular signature of EVs mirrors the pathophysiological status of their originating cells, thus enabling the bioactive EV cargo to serve as a biomarker for early disease detection.⁷ EVs are known to play a central role in the pathological dissemination of cancer,⁸ CVD,⁹ and neurodegeneration.¹⁰ Recently, CKD-derived EVs were shown to induce smooth muscle cell calcification¹¹ and vascular remodeling,¹² and several EV microRNA (miRNA) signatures discovered in a rodent model of CKD have been linked to vascular calcification.¹¹ Nonetheless, significant knowledge gaps remain about whether circulating CKD-EVs from kidneys directly affect cardiomyocyte (CM) and cardiac function, as well as the mechanism by which CKD-EVs cause HF in patients with CKD.

Our goal in this study was to characterize the molecular underpinnings of EV-mediated pathological communication from the kidney to the heart in patients with CKD. To address this, we: (1) collected plasma samples from patients with CKD and healthy controls and from a CKD mouse model of HF; (2) evaluated the direct cardiotoxic effects of circulating/kidney-derived CKD-EVs on human and rodent CMs in vitro and mice hearts in vivo; (3) investigated the impact of CKD-EVs on CM and cardiac contractile functions both in vitro and in vivo; (4) used small RNA sequencing to identify the miRNA cargo responsible for CKD-EV cardiotoxicity and validated the

Chronic kidney disease (CKD) is increasingly recognized as a major global public health concern, affecting >800 million individuals and resulting

function of CKD-EV-miRNA risk factors in CM apoptosis and contractility; and (5) determined the renal and cellular origins of cardiotoxic CKD-EV-miRNAs. Our findings have the potential to define cardiotoxic CKD-EV contents as biomarkers in early diagnosis of and novel therapeutics for HF in patients with CKD.

METHODS

Data supporting the findings of this study are available from the corresponding author upon reasonable request. Expanded methods are provided in the [Supplemental Material](#).

Study Design

This study aimed to investigate the role of circulating EVs in the pathogenesis of HF in patients with CKD. We first compared plasma EVs from patients with CKD (hCKD-EVs) to plasma EVs from healthy controls (hCtr-EVs) to evaluate cardiotoxic function in cardiac cell death and contractile dysfunction, both *in vitro* and *in vivo*. To gain mechanistic insights and to define EV-mediated kidney-cardiac pathological communication, we used a mouse model of adenine diet–induced CKD that instigated HF with reduced cardiac function. Molecular cargo of hCKD-EVs was identified by small RNA sequencing and quantitative reverse transcription polymerase chain reaction (qRT-PCR), and the top differentially expressed miRNAs were functionally quantified by using human AC16 (hAC16) CMs and human induced pluripotent stem cell–derived (hiPSC) CMs. The renal and cellular origins of cardiotoxic CKD-EV-miRNAs were determined from the corresponding endogenous primary miRNA (pri-miRNA) expressions in different tissues and kidney cells in CKD or control (Ctr) mice.

Human Subjects

The study was approved by the institutional review boards of the Mount Sinai Hospital and the University of Virginia (approval HSR#20550). The participants gave written informed consent. Blood samples were collected from patients with moderate or advanced CKD and healthy controls ([Tables S1 and S2](#)). History of CKD was defined based on patient's medical history and hospital records. In the cohort of patients with CKD, participant inclusion used the following criteria: (1) outpatients at University of Virginia Medical Center nephrology clinic from 2018 to 2025, (2) >18 years of age, and (3) CKD diagnosed according to the Kidney Disease Improving Global Outcomes guidelines,¹³ based on cause, glomerular filtration rate categories (G1–G5), and albuminuria. Kidney Disease Improving Global Outcomes defines CKD as abnormalities of kidney structure or function, present for a minimum of 3 months, with implications for health. Subjects with heart transplant were excluded. Blood from patients receiving hemodialysis was obtained before dialysis treatment. The following were exclusion criteria for all subjects: active infections, active malignancy, immunomodulatory therapy, bleeding disorder, pregnancy/nursing, sickle cell disease, or anemia. Healthy control subjects had no chronic conditions and were recruited based on clinical history and self-report. In this proof-of-concept study, our sample size was based on availability of patient and control samples rather than formal power calculations.

Statistical Analysis

Groups were first assessed for normality to determine whether parametric or nonparametric tests would be used. Assumptions of normality were tested with the Shapiro-Wilk test. The Levene test was used for equality of variances. Normally distributed data with equal variances were statistically analyzed with either 2-tailed Student *t* test (2 groups) or 1-way ANOVA (3 or more groups with one experimental factor) with Tukey multiple comparison test or Dunnett multiple comparison test. Normally distributed data with 2 experimental factors were analyzed with 2-way ANOVA followed by pairwise comparisons with Tukey multiple comparison test. Nonnormally distributed data were analyzed using Mann-Whitney *U* test (2 groups) or Kruskal-Wallis test (3 or more groups). Grubbs test was used to detect outliers. All data are shown either as the mean \pm SEM (normally distributed data) or median \pm interquartile range (not normally distributed data). For human subject characteristics, data are given as median with interquartile range for all. *P* value is calculated using the nonparametric Kruskal-Wallis test. To evaluate the association between miRNA expression and HF biomarkers, a Pearson correlation analysis on log-transformed data was performed. All data were graphed using Prism 9 (GraphPad software, version 9.5.0) or R, and statistical analyses were performed in Prism 9 or R. The statistical details, sample size, and significance levels for each experiment are specified in the figure legends.

RESULTS

Study Population

The functional and pathological roles of circulating hCKD-EVs in reno-cardiac communication, cardiac contractility, remodeling, and HF have not been studied. To investigate these dynamics, we recruited 35 well-characterized patients with CKD with stable moderate or advanced CKD (stages 3–5) plus 18 comparable healthy controls ([Tables S1 and S2](#)). Compared with healthy controls, the CKD cohort had significantly lower median estimated glomerular filtration rate and significantly higher urinary albumin to creatinine ratio levels, thus indicating impaired renal function. Demographics, patient characteristics, and other risk factors like obesity, uncontrolled hypertension, and diabetes did not significantly differ between the CKD and control groups. All patients with CKD received guideline-directed medical therapy to ensure standardized therapeutic interventions across the cohort. All patients with CKD were in a steady state, with no ongoing acute kidney injury. Higher medication use within the CKD cohort reflected the intense therapeutic regimen necessitated by their disease state.

Circulating hCKD-EVs Induce CM Apoptosis and Contractile Dysfunction

We collected plasma samples from patients with moderate or advanced CKD (stages 3–5) and healthy

controls. Because larger microvesicles in plasma have been shown to have platelet or erythrocyte origins,^{14,15} we focused on smaller EVs. To this end, small EVs were isolated from platelet-poor and microvesicle-depleted human plasma by using ultracentrifugation, a precipitation or size exclusion chromatography method, as previously described^{16,17} (Figure 1A; Figure S1). Plasma hCKD-EVs versus hCtr-EVs did not significantly differ in either size (≈ 90 nm versus ≈ 97 nm, respectively, determined using dynamic light scattering; Figure 1B) or concentration (quantified using nanoparticle tracking analysis; Figure S2A to S2C). Western blot determined the presence of EV-surface marker proteins flotillin 1, CD63, and CD81, as well as EV intraluminal marker protein Alix (Figure 1C) and the absence of EV-negative marker GM130 (Figure S2D), thus confirming EV purity. Single EV phenotyping by nano-flow cytometry revealed known EV-surface tetraspanin marker proteins (CD9, 63, and 81; Figure 1D), plus a significantly increased number of tetraspanin^{+ve} (tetraspanin-positive) hCKD-EVs compared with hCtr-EVs (Figure 1D; Figure S3), consistent with the literature.^{18,19} Cryo-electron microscopy (Figure 1E) showed the presence of EVs with known nano-size and morphology. Our EV characterization data confirmed successful isolation of EVs from human plasma of patients with CKD and healthy controls.

To investigate hCKD-EV cardiotoxicity, we separated platelet- and microvesicle-free CKD plasma into EV-enriched or EV-depleted fractions, treated each fraction (20 µg protein equivalent to 1.6e9 particles/100 µL for EVs) with hAC16-CMs in culture, and then compared cell viability between the fractions after 48 hours (Figure 1F). It is interesting that hCKD-EVs, but not the hCtr-EVs, hCKD-EV-depleted fractions, or hCtr-EV-depleted fractions, significantly decreased hAC16-CM viability *in vitro* (Figure 1F). These data suggest that circulating hCKD-EVs are a key cardiotoxicity mediator in plasma of patients with CKD.

Further characterization of the cardiotoxic effects of hCKD-EVs shows significant increases in hAC16-CM death and Terminal deoxynucleotidyl transferase dUTP nick end labeling (TUNEL)-positive apoptotic cells treated with hCKD-EVs compared with hCtr-EVs (Figure 1G through 1K). To study if hCKD-EVs impact CM function, we treated adult rat primary CMs with hCKD-EVs or hCtr-EVs and quantified their contractile function and Ca²⁺ handling by using the IonOptix Myocyte Calcium and Contractility System (Figure 1G). IonOptix analysis demonstrated that compared with hCtr-EVs, hCKD-EVs significantly impair contractile function and Ca²⁺ handling in adult primary CMs (Figure 1L and 1M; Figure S4). Next, to evaluate hCKD-EVs cardiotoxicity *in vivo*, we administered hCKD-EVs or hCtr-EVs (100 µg/8e9 particles) to the left ventricle (LV) of non-obese diabetic mice with severe combined immunodeficiency (NOD/Scid) mice through intramyocardial injection (Figure 1N).

Troponin^{+ve} CMs internalized PKH67-labeled hCKD-EVs (Figure 1O). Administration of hCKD-EVs, compared with hCtr-EVs, significantly expanded TUNEL-positive apoptotic cells in the LV (Figure 1P and 1Q). Taken together, these data suggest that circulating plasma EVs from patients with CKD detrimentally affect CM viability, contractile function, and Ca²⁺ handling.

Mouse Adenine Diet-Induced CKD Model Led to HF

To investigate the role of kidney-derived EVs in the pathogenesis of CKD-induced HF, we used a previously reported adenine (Ade) diet-induced CKD mouse model of reno-cardiac syndrome.²⁰ This model mimics the pathophysiology of human CKD-induced HF, with tubular and glomerular damage as well as interstitial fibrosis. However, varying amounts of adenine in the diet generate different levels of cardiomyopathy.²¹ To study the pathomechanism of reno-cardiac disease, we used a 0.25% adenine diet to create severe CKD, which was sufficient to induce cardiac dysfunction. Our CKD mouse model developed HF at 8 weeks. We thoroughly characterized the HF phenotype by assessing cardiac function, hypertrophy, fibrosis, and biochemistry at 4 weeks and 8 weeks by performing echocardiogram, magnetic resonance imaging, and histology (Figure 2A).

CKD mice exhibited significantly higher plasma blood urea nitrogen and creatinine level, increased blood pressure, early signs of systolic dysfunction at 4 weeks (Figure S5), and established HF at 8 weeks (Figure 2B; Figure S6). Cardiac magnetic resonance imaging revealed CKD mice had depressed LV systolic function with distinctly reduced LV longitudinal strain and mitral annular plane systolic excursion (Figure 2C and 2D; Figure S6F). In agreement, echocardiogram analysis showed significantly worsened LV systolic dysfunction (quantified by LV ejection fraction and LV fractional shortening) in CKD mice (Figure 2E). Echocardiogram and magnetic resonance imaging data also demonstrated substantial LV dilatation and hypertrophy with higher LV end-diastolic and LV end-systolic volumes ($P=0.06$); thicker LV anterior and posterior walls; indexed LV mass, septal, and lateral walls; expanded relative wall thickness; and right ventricle dysfunction in CKD mice (Figure S6D through S6I). Histological data confirmed adverse cardiac remodeling in CKD mice with significantly more fibrosis in both the kidney (Figure S6B) and heart (Figure S6C), and increased CM size and area indicating hypertrophy (Figure 2F). In addition, LV tissues from CKD hearts had elevated markers of HF (BNP and atrial natriuretic peptide [ANP]), fibrosis (measured by Sircol and hydroxyproline assays), oxidative stress (higher malondialdehyde and lower activity of the antioxidant enzyme superoxide dismutase), and apoptosis (caspase-3 activity; Figure S7).

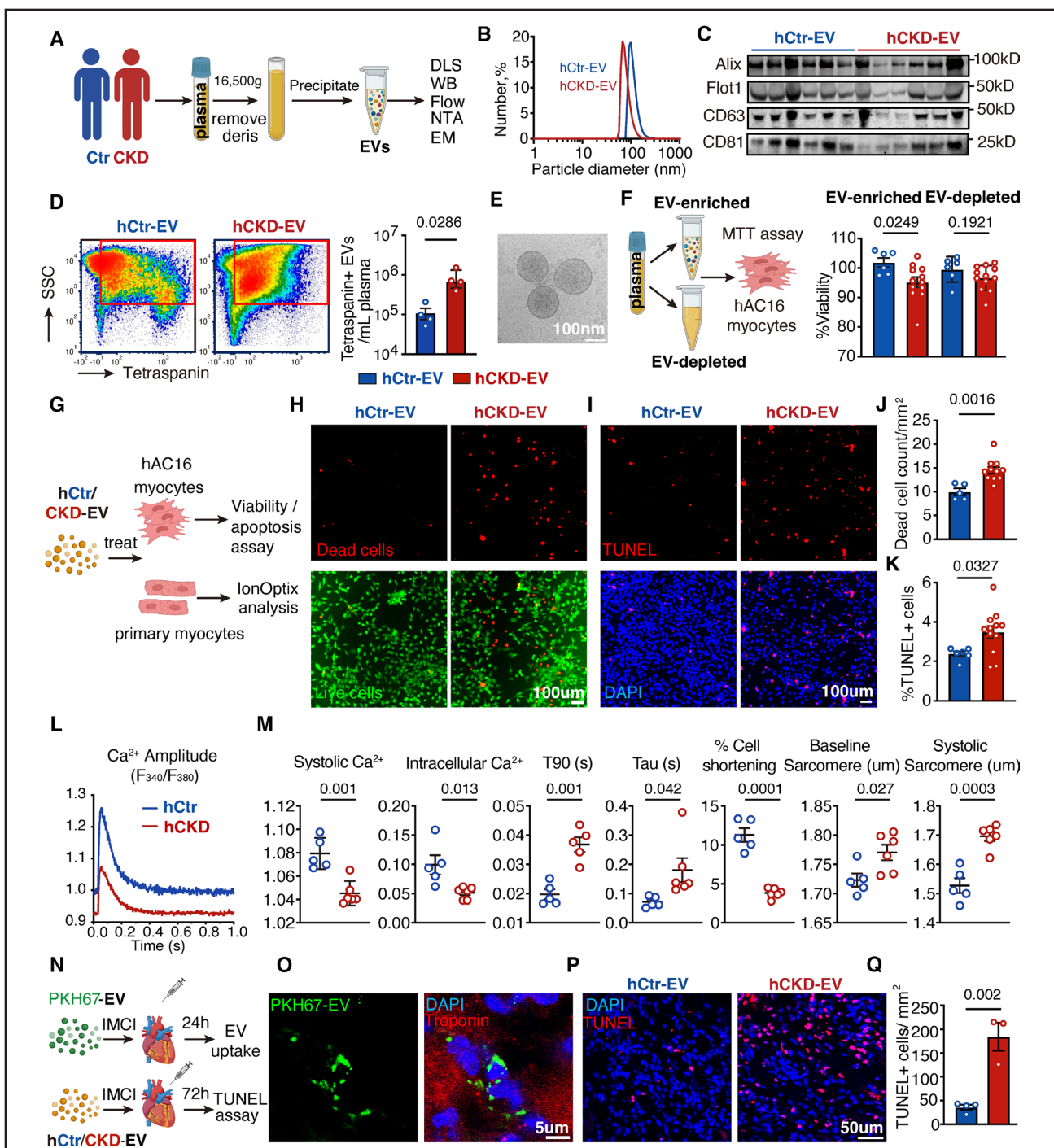


Figure 1. Circulating hCKD-EVs are cardiotoxic *in vitro* and *in vivo*.

A, Study design for EV isolation and characterization. **B**, Dynamic light scattering (DLS) analysis of EV size. **C**, Western blotting (WB) of EV-positive markers (Alix, Flot1, CD81, and CD63) for EVs ($n=6$). **D**, Nanoflow cytometry analysis of tetraspanins (CD9, CD63, and CD81) for EVs ($n=3$). **E**, Cryo-electron microscopy (EM) of human plasma EVs. **F**, Viability of hAC16-CMs treated with equal amounts of protein (200 μ g/mL) from EV-enriched or EV-depleted plasma after 48 hours ($n=6-12$) using MTT (3-(4,5-dimethylthiazol-2-yl)-2,5-diphenyltetrazolium bromide) assay. **G**, Study design for EV functional analysis in vitro. **H** and **I**, Representative image of live/dead assay and Terminal deoxynucleotidyl transferase dUTP nick end labeling (TUNEL) assay of hAC16-CMs treated with hCKD-EVs and hCtr-EVs. **J** and **K**, Quantification of live/dead assay and TUNEL assay ($n=5-12$). **L** and **M**, IonOptix analysis showing calcium transients and contractility of rat primary cardiomyocytes treated with hCKD-EVs and hCtr-EVs ($n=5$ or 6). **N**, Study design for EV functional analysis in vivo. **O**, Intramyocardial injection (IMCI) of hCKD-EVs labeled with PKH67 dye showing EV uptake in NOD/Scid mice heart. **P**, Representative image of TUNEL assay in NOD/Scid hearts injected with hCKD-EVs and hCtr-EVs. **Q**, Quantification of TUNEL⁺ cells in mice hearts injected with hCKD-EVs or hCtr-EVs ($n=3$ or 4). Data in **D** are presented as median with interquartile range and were analyzed with Mann-Whitney *U* test. Data in **F**, **J**, **K**, **M**, and **Q** are presented as mean \pm SEM and were analyzed using Student *t* test. CKD indicates chronic kidney disease; Ctr, control; EVs, extracellular vesicles; hCKD-EV, plasma EVs from patients with CKD; hCtr-EV, plasma EVs from healthy controls; NTA, nanoparticle tracking analysis; and SSC, side scatter.

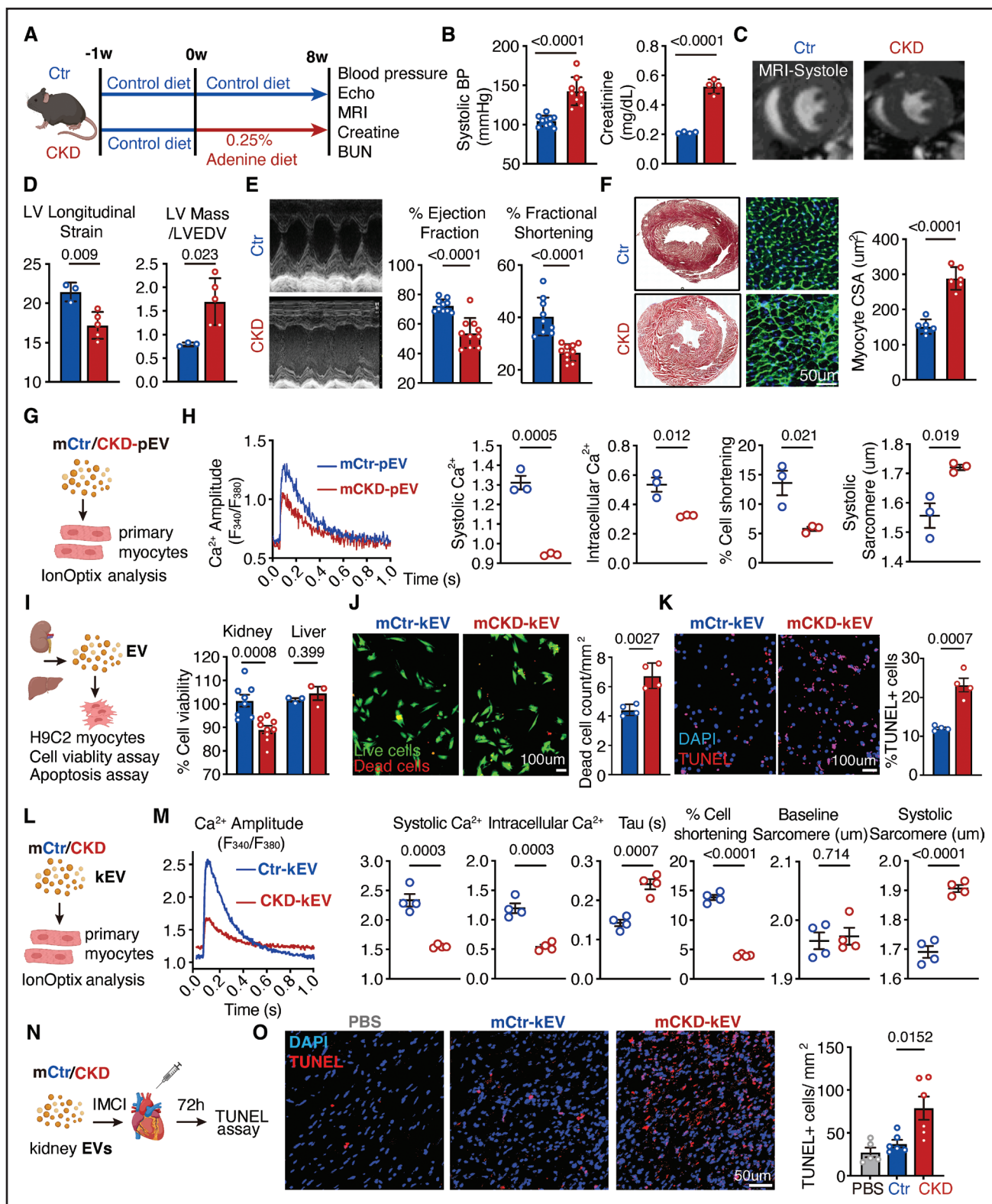


Figure 2. Adenine-induced CKD mouse model shows heart failure and EVs from Ade-CKD mice are cardiotoxic.

A, Generation of CKD mouse model. **B**, Quantification of systolic blood pressure (BP; n=9) and creatinine (n=4) in Ade-CKD (red) and control (Ctr; blue) mice at 8 weeks. **C** and **D**, Magnetic resonance imaging (MRI) quantification of LV longitudinal strain and LV mass/LV end-diastolic volume (LVEDV) ratio at 8 weeks (n=3–5). **E**, Echocardiographic quantification of percent ejection fraction (EF) and percent fractional shortening (FS) to assess cardiac function at 8 weeks (n=10). **F**, Masson trichrome staining of LV showing fibrosis and wheat germ agglutinin (WGA) staining showing hypertrophy in CKD vs Ctr mice at 8 weeks (n=6). **G**, Schematic of mouse plasma EV (mCtr/CKD-pEV) functional study. **H**, Representative calcium amplitude transients through one contraction-relaxation cycle of rat primary cardiomyocytes treated with (Continued)

Figure 2 Continued. mCtr/CKD-pEV as measured by IonOptix analysis. Quantification of calcium transients and contractility in primary cardiomyocytes treated with mCtr/CKD-pEV ($n=3$). **I**, Viability of H9C2 cells treated with equal protein amounts of Ctr/CKD kidney-derived ($n=8$ or 9) or liver-derived ($n=3$) EVs. **J** and **K**, Live and dead cell assay and Terminal deoxynucleotidyl transferase dUTP nick end labeling (TUNEL) assay of H9C2 cells treated with mCtr-kEVs or mCKD-kEVs ($n=4$). **L**, Schematic of IonOptix analysis of rat primary CMs treated with mCtr/CKD-kEVs. **M**, Representative calcium amplitude transient through one contraction-relaxation cycle, and quantification of calcium transients and contractility of primary CMs treated with mCtr/CKD-kEVs as measured by IonOptix analysis ($n=4$). **N**, Schematic of mCtr/CKD-kEVs functional assays in vivo. **O**, Representative image of TUNEL assay of C57BL/6J mouse hearts injected with equal protein from mCKD-kEVs and mCtr-kEVs. Quantification of TUNEL⁺ cells in mice hearts injected with mCtr/CKD-kEVs ($n=3$ or 4). Data are presented as mean \pm SEM and were analyzed using the Student *t* test. BUN indicates blood urea nitrogen; CKD, chronic kidney disease; CSA, cross-sectional area; EVs, extracellular vesicles; IMCI, intramyocardial injection; LV, left ventricle; and PBS, phosphate-buffered saline.

Circulating Plasma and Kidney Tissue-Derived EVs From CKD Mice Are Cardiotoxic

To test the role of circulating EVs in HF in CKD mice, we isolated plasma EVs from CKD mice (mCKD-pEVs) and control mice (mCtr-pEVs) at 8 weeks by using the precipitation method (Figure S8A). The EV-marker proteins Alix and flotillin 1 had significantly higher expression in mCKD-pEVs compared with mCtr-pEVs (Figure S8B), whereas the size distribution and total particle counts were comparable (Figure S8C and S8D). To assess cardiotoxicity, we treated isolated adult rat primary CMs with either mCKD-pEVs or mCtr-pEVs and then quantified their contractile function (Figure 2G). Similar to hCKD-EVs from patients, mCKD-pEV treatment significantly decreased systolic and intracellular Ca^{2+} and percent cell shortening and increased systolic sarcomere length in adult rat primary CMs compared with mCtr-pEV treatment (Figure 2H). These data suggest that mCKD-pEVs are cardiotoxic and induce contractile dysfunction in primary CMs in vitro.

Next, to examine whether CKD-kidney-derived EVs directly affect the heart, we isolated kidney-EVs from digested, cell-free kidney supernatants of both 8-week CKD and control mice by using a modified tissue-EV isolation protocol.²² Debris and contamination originating from intracellular sources were removed by floating the EVs up through an iodixanol density gradient ultracentrifugation (Figure S9). Kidney-derived EVs from both CKD mice (mCKD-kEVs) and control mice (mCtr-kEVs) were \approx 80 to 100 nm in size (Figure S10A and S10B), positive for EV markers (Alix and flotillin 1), and negative for a known non-EV marker (Cytochrome c1 [Cyc1]; Figure S10C), thus demonstrating purity. It is interesting that mCKD-kEVs had significantly more EV marker protein Alix (quantified from Western blot; Figure S10C), a higher percentage of tetraspanin-positive EVs (quantified by single-EV flow cytometry, Figure S10E), but significantly fewer total particles per kidney (measured by nanoparticle tracking analysis; Figure S10D). These results suggest mCKD-kEVs qualitatively and quantitatively differ from mCtr-kEVs.

When administered (10 μg , \approx 1.2e10 particles/100 μL) to rat myocytes (H9C2 cells)²³ in culture, mCKD-kEVs significantly lowered their viability compared with mCtr-kEVs, thus indicating the cardiotoxic effects of mCKD-kEVs (Figure 2I). In contrast, mCKD-liver-EVs from CKD

mice were not cardiotoxic (Figure 2I), suggesting the cardiotoxicity is limited to the CKD kidney EVs. Moreover, in live and dead and TUNEL assays, mCKD-kEVs significantly induced H9C2 cell death and apoptosis compared with mCtr-kEVs (Figure 2J and 2K). Our IonOptix analysis of adult rat primary CMs showed that mCKD-kEVs significantly impaired adult rat primary CMs contractility and Ca^{2+} handling compared with mCtr-EVs (Figure 2L and 2M). mCKD-kEVs injected intramyocardially into mice hearts (20 μg [\approx 2.4e10 particles]/injection) were taken up by cardiac cells and significantly increased the apoptosis compared with mCtr-kEVs (Figure 2N and 2O). Taken together, these findings illustrated that kidney-derived EVs exert direct cardiotoxic effects on both CMs and the heart.

Depleting Circulating EVs Ameliorated HF in a CKD Mouse Model

To verify if circulating CKD-EVs contribute to the pathogenesis of HF in vivo, we depleted circulating EVs in CKD mice by injecting them with GW4869 (GW), a systemic inhibitor of neutral sphingomyelinase, an enzyme involved in EV biogenesis,^{11,24,25} for 10 weeks (Figure 3A). Circulating particle numbers significantly decreased and tetraspanin⁺ EV numbers dropped to less than half in both kidney and plasma of GW-injected CKD mice compared with vehicle-injected CKD mice (Figure 3B; Figure S11). Neither blood urea nitrogen level nor blood pressure was altered in either GW- or vehicle-injected CKD mice, and both remained elevated compared with controls (Figure 3C and 3D). In contrast, plasma creatinine level dropped significantly in GW-CKD mice compared with vehicle-CKD mice and was significantly higher than in GW-Ctr mice (Figure 3C), thus indicating the kidney injury in GW-CKD mice (Figure 3C and 3D). It is remarkable that cardiac function, as measured by percent ejection fraction and percent fractional shortening, was substantially improved in the GW-CKD mice compared with vehicle-CKD mice (Figure 3E and 3F). In addition, GW-CKD mice showed significantly ameliorated cardiac fibrosis (Figure 3G) and hypertrophy (Figure 3E through 3H). The heart-to-body weight ratio was significantly decreased in GW-CKD mice compared with vehicle-CKD mice (Figure S11D). Results from this loss-of-function experiment demonstrated that depleting CKD-EVs rescues cardiac function even in the presence of kidney injury, high blood pressure, and other comorbidities

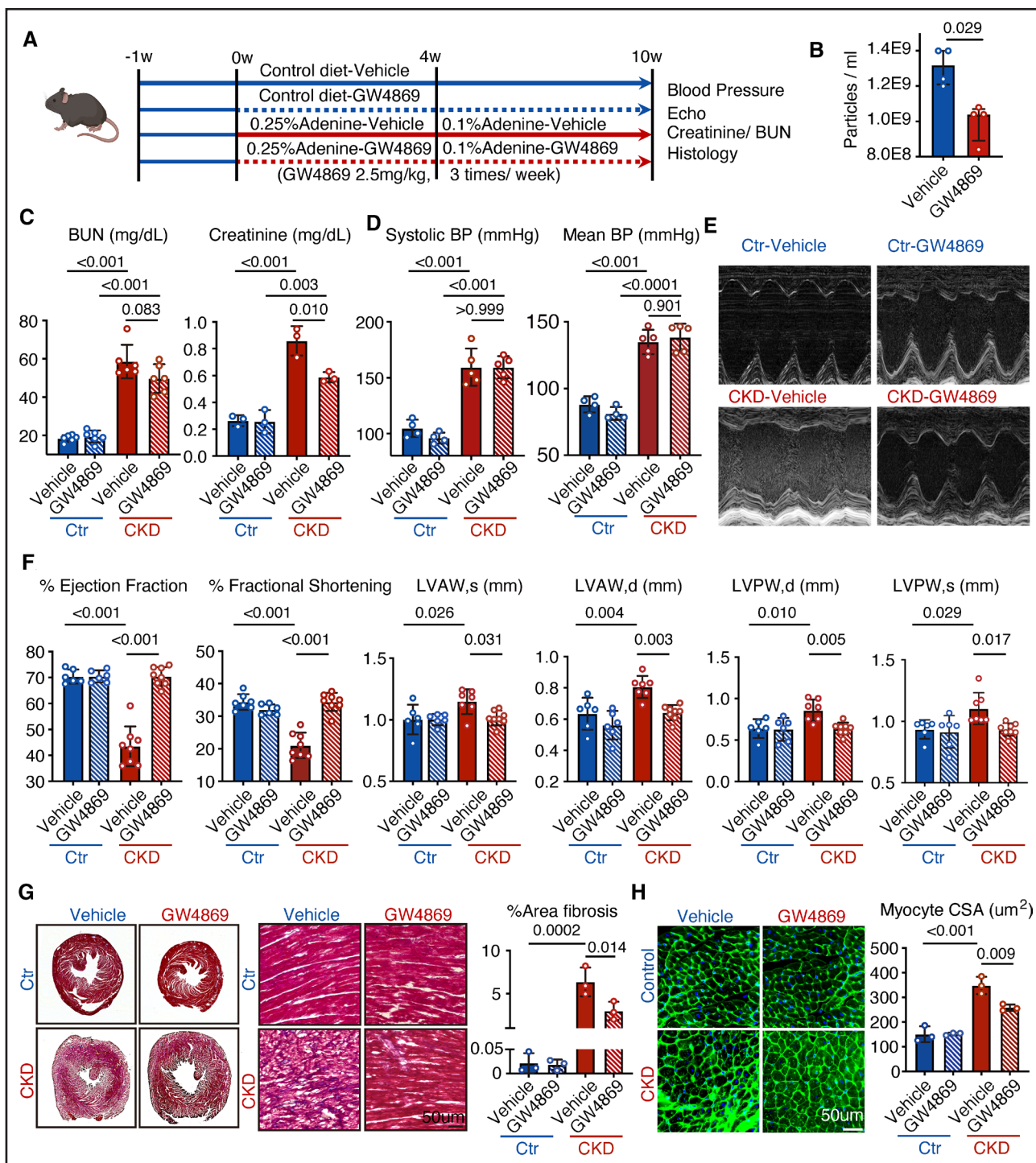


Figure 3. Depletion of EVs improves cardiac function in CKD mice.

A, Schematic of study design. C57BL/6J mice fed an adenine diet received an intraperitoneal injection of 2.5 mg/kg (3 times/week) of either GW4869 or vehicle (7.5% DMSO in saline) for 10 weeks. **B**, Quantification of mouse plasma particle counts from CKD mice receiving either vehicle or GW4869 as measured by nanoparticle tracking analysis (NTA; n=4). **C** and **D**, Measurement of blood urea nitrogen (BUN), plasma creatinine level, and systolic and mean blood pressure in Ctr and CKD mice treated with either vehicle or GW4869. **E**, Echocardiographic image of ventricle wall motion in Ctr and CKD mice treated with either vehicle or GW4869. **F**, Echocardiography of heart function showing %EF, %FS, and wall thickness (n=10), groups as indicated. **G**, Representative Masson-trichrome staining of cross-sections of the whole heart and LV, and quantification of percent fibrosis in the groups as indicated (n=3). **H**, WGA staining and quantification of myocyte cross-sectional area (CSA) of the hearts from the groups as indicated (n=3). Data are presented as mean±SEM. Data in **B** are presented as median with interquartile range and were analyzed with Mann-Whitney *U* test. Data in **C** through **H** were analyzed using 2-way ANOVA followed by Tukey multiple comparison test. CKD indicates chronic kidney disease; CSA, cross-sectional area; Ctr, control; LVAW, LV anterior walls; and LVPW, LV posterior walls.

circulating in the plasma. Our data therefore established that circulating CKD-EVs play a causal role in and significantly contribute to CKD-induced HF.

Circulating EVs From Patients With CKD Carry a Distinct microRNA (miRNA or miR) Signature

The molecular components of hCKD-EVs that are responsible for cardiac dysfunction are largely unknown. EVs are selectively enriched for small RNAs that can provide mechanistic insights into HF pathogenesis and progression in patients with CKD. To identify CKD-EV risk factors, we examined the transcriptomic profiles of hCKD-EV-RNA (from 13 patients with CKD) and compared them with hCtr-EV-RNA (from 6 healthy subjects) by using deep small RNA sequencing followed by qRT-PCR validation (Figure 4A).

Principal component analysis revealed that the miRNA expression profiles of cardiotoxic hCKD-EVs were distinct from those of noncardiotoxic hCtr-EVs (Figure 4B). The clustered hCtr-EVs exhibited low variability, whereas the hCKD-EVs displayed irregular distributions, both clustering with hCtr-EVs and showing discrete patterns, suggesting the heterogeneity within the CKD group (Figure 4B).

The transcriptomic profiles of hCtr-EVs and hCKD-EVs differed significantly, as depicted in the volcano plot (Figure 4C; $P<0.05$; log-fold change >1.0), heatmap (Figure 4D), and list of top 51 differentially expressed miRNAs (Figure S12). For further validation, we selected: (1) 10 upregulated miRNAs exhibiting the highest significant log-fold changes (miR-320a-3p, 4454, and 2110) and most abundant expression levels (miR-22-5p, 423-5p, 320b, 484, 193a-5p, 130b-3p, and 378a-3p) in hCKD-EVs (Figure 4E); and (2) 4 downregulated miRNAs common between our differentially expressed list and previously reported downregulated CKD miRNAs^{11,12} conserved between species (Figure S12 and S13). Of note, the only study with unbiased small RNA sequencing of clinical CKD-EV samples (from children after kidney transplant) reported mostly downregulated miRNAs. Kyoto Encyclopedia of Genes and Genomes analysis showed the significantly enriched pathways, including apoptosis, autophagy, and cell senescence (Figure 4F), a result that aligns with the proapoptotic and cardiotoxic properties of the hCKD-EVs. Our qRT-PCR validation confirmed that 9 of the 10 upregulated miRNAs (miR-130b-3p, 193a-5p, 2110, 22-5p, 320a-3p, 320b, 378a-3p, 423-5p, and 484) had significantly higher expression in hCKD-EVs than in hCtr-EVs, whereas miR-4454 remained unchanged. qRT-PCR analysis also confirmed significant downregulation of 2 CKD-EV-miRNAs (miR-142-5p and 17-5p) and no change in the other 2 miRNAs (miR-224-5p and 16-5p) compared with hCKD-EVs (Figure 4G).

To examine differences between patients with CKD with and without HF (CKD[+]HF and CKD[-]HF) in their

miRNA expressions, we compared miRNA levels in their plasma EVs. It is interesting that expression of several CKD-miRNAs (130-3p, 2110, 320a-3p, 320b, 378a-3p, and 423-5p) was significantly higher in EVs from both CKD(+)HF and CKD(-)HF patients compared with Ctr but was comparable between these 2 patient groups (Figure S14). The lack of significant difference between CKD(-)HF and CKD(+)HF could be a result of the fact that the CKD(-)HF group (percent ejection fraction >50 ; Table S2) is heterogeneous and likely includes patients with heart failure with preserved ejection fraction or subclinical or asymptomatic HF. To confirm this, we assayed for ANP, NT-proBNP (N-terminal pro-B-type natriuretic peptide), and hsTNI (high-sensitivity Troponin I), known markers of myocardial injury and HF, in CKD(-)HF, CKD(+)HF groups and healthy Ctr groups using quantitative immunoassays (similar to those in clinics). It is remarkable that all 3 markers were significantly higher in plasma of both CKD(+)HF and CKD(-)HF cohorts compared with healthy Ctr (Figure S15), suggesting the presence of cardiac stress and subclinical HF in the CKD(-)HF cohort. Moreover, expression of many (9 of the total 14 tested) CKD-EV-miRNAs correlated with these HF markers (Figure S16 through S18), thus underscoring the need to analyze a well-characterized population of patients with CKD for novel biomarker and therapeutic target discovery for HF.

miRNAs Enriched in hCKD-EVs Are Cardiotoxic to Human CMs

To test whether the above miRNAs enriched in hCKD-EVs are cardiotoxic, we treated hAC16-CMs and hiPSC-CMs with 9 miRNA mimics and quantified their effects on viability and contractility by using the MTT (3-(4,5-dimethylthiazol-2-yl)-2,5-diphenyltetrazolium bromide) assay and IonOptix measurements, respectively. The MTT assay revealed that 4 miRNA mimics (miR-2110, 320b, 484, and 130b-3p) significantly decreased hAC16-CMs viability (Figure 5A). IonOptix analysis of beating hiPSC-CMs showed that 7 miRNA mimics (miRs-2110 and 320b [both human-specific], 484, 130b-3p, 193-5p, 22-5p, and 320a-3p) significantly reduced intracellular Ca^{2+} , and 4 of these also lowered the systolic Ca^{2+} (Figure 5B and 5C; Figure S19), compared with control-miRNA mimic treatment. In addition, these miRNA mimics significantly increased the time for the Ca^{2+} signal (fluorescence intensity F; F_{340}/F_{380}) to rise from 10% to 90% and time constant for calcium decay in treated hiPSC-CMs. In addition, inhibition of downregulated CKD-EV-miRs by using anti-miR-142-5p and anti-miR-17-5p did not affect hAC16-CM viability. However, anti-miR-17-5p significantly reduced Ca^{2+} transients in treated hiPSC-CMs (Figure S20), thereby demonstrating the cardioprotective function of downregulated CKD-EV-miRNAs. These findings suggest that the miRNAs enriched in hCKD-EVs are cardiotoxic to human CMs in vitro.

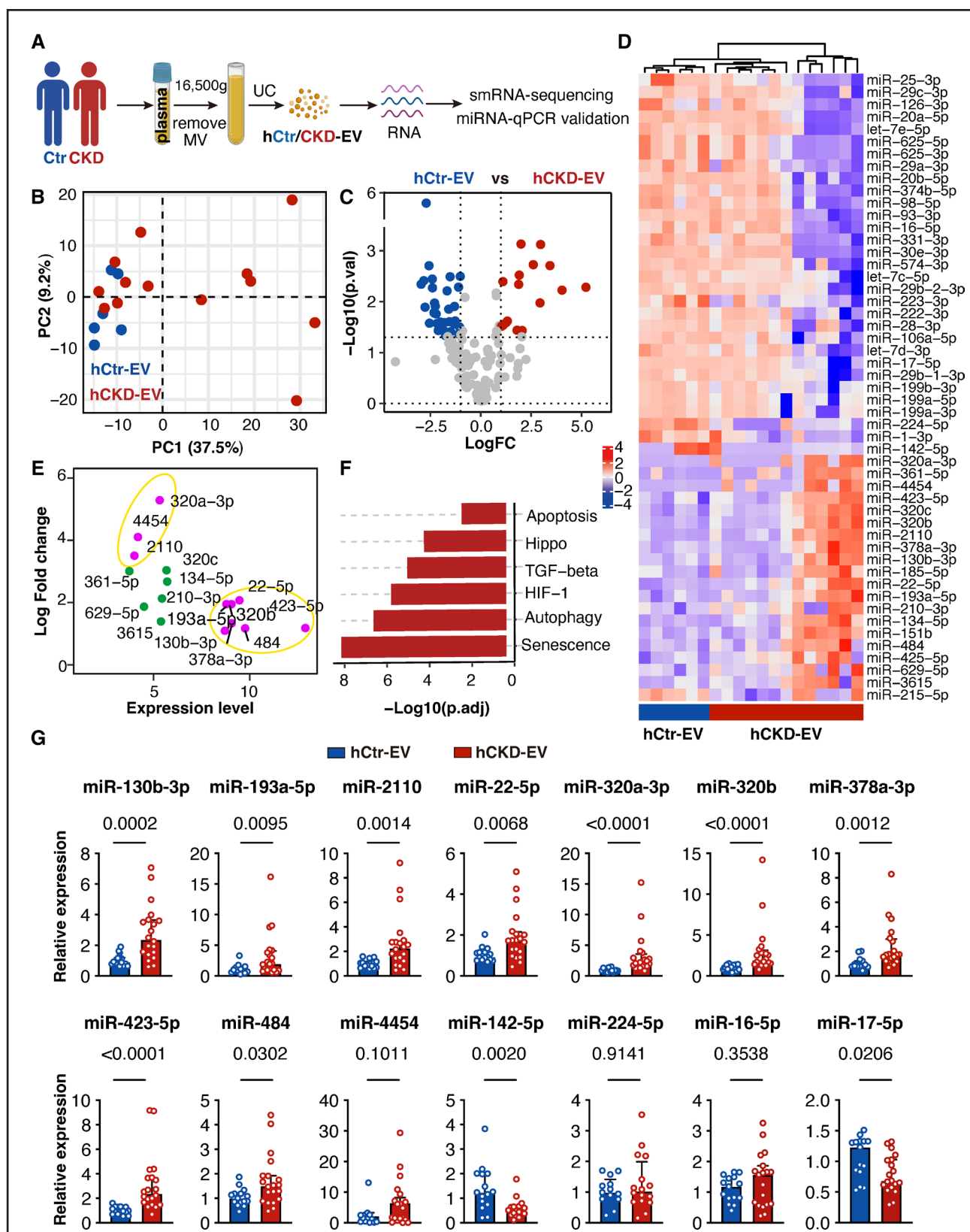


Figure 4. microRNA (miR) signatures of human plasma CKD-EVs.

A, Schematic of study design. **B**, Principal component analysis (PCA) of miRNA sequencing data from hCtr/CKD-EVs. **C** and **D**, Volcano plot and heatmap showing differentially expressed miRNAs in hCKD-EVs compared with hCtr-EVs (control, n=6; CKD, n=13). Sixteen upregulated and 36 downregulated miRNAs in hCKD-EVs were identified. **E**, Analysis of significantly expressed miRNAs with high log-fold change and high abundance in hCKD-EVs compared with hCtr-EVs. Among the 16 upregulated miRNAs in hCKD-EVs, 3 exhibited the highest (Continued)

Figure 4 Continued. log-fold changes (miR-320a-3p, 4454, and 2110), and 7 (miR-22-5p, 423-5p, 320b, 484, 193a-5p, 130b-3p, and 378a-3p) showed the most abundant expression in hCKD-EVs. **F**, KEGG pathway analysis showing the top 6 most enriched pathways in highly expressed hCKD-EV-miRNAs. **G**, qRT-PCR analysis of miRNA expressions in hCKD-EVs compared with hCtr-EVs (Ctr, n=15; CKD, n=20). Data in **D** are present as median with interquartile range and were analyzed with Mann-Whitney *U* test. CKD indicates chronic kidney disease; CSA, cross-sectional area; Ctr, control; EVs, extracellular vesicles; hCKD-EV, plasma EVs from patients with CKD; hCtr-EV, plasma EVs from healthy control; MV, microvesicles; smRNA, small RNA; and UC, ultracentrifugation.

To determine whether CMs effectively internalized hCKD-EVs to subsequently increase miRNA expression, we treated hAC16-CMs with hCKD-EVs and studied first EV uptake and then miRNA expression (Figure 5D). Uptake analysis of PKH67 dye-labeled hCKD-EVs confirmed their internalization into the cytoplasm of hAC16-CMs after 4 hours of treatment in vitro (Figure 5E). PKH67-hCKD-EVs intravenously injected into mice through a tail vein (Figure S21A) showed higher cardiac uptake than dye-only control injections, as determined using in vivo imaging system (Figure S21B). Immunofluorescence analysis showed the PKH67-hCKD-EVs were internalized by troponin^{+ve} CMs in the heart (Figure S21C). These data indicate that CMs take up the CKD-EVs both in vitro and in vivo. To study whether CKD-EV internalization induces CKD-miRNA expression, we incubated equal numbers of hCtr- or hCKD-EVs with hAC16-CMs (2e5 particles per cell) for 4 hours and then measured cellular miRNA expression. qRT-PCR quantification revealed that 4 miRNAs (miR-2110, 320b, 130b-3p, and 484) had significantly upregulated expression in hCKD-EV-treated cells compared with hCtr-EV-treated cells (Figure 5F), thereby corroborating effective EV internalization. It is interesting that expression of another 5 miRNAs remained unchanged between hCKD-EV- and hCtr-EV-treated cells (Figure 5G), a finding that suggests these miRNAs have either lower abundance in hCKD-EVs or higher endogenous levels in hAC16-CMs. Collectively, these data demonstrate that CMs can internalize miRNA-carrying hCKD-EVs that contribute to the cardiotoxicity through proapoptotic effects and by disrupting CM contractility and Ca²⁺ handling.

Some of the novel enriched cardiotoxic miRNAs in CKD-EVs (eg, miR-2110 and miR-320b) are human-specific and have not previously been characterized for function on CMs. To determine their function in response to CKD-EVs, we used antisense oligonucleotides (anti-miRs) that bind to target miRNAs and negate the function of CKD-EVs carrying those miRNAs. Specifically, we treated hAC16-CMs with each anti-miRNA followed by cotreatment with CKD-EVs, which suppressed EV-miRNA activity. As expected, hAC16-CMs cotreated with CKD-EVs and a scrambled control anti-miR showed significantly reduced viability. It is remarkable that cotreating CKD-EVs with anti-miRs-2110/320b improved cell viability (Figure 5H; Figure S22). These data demonstrate that EV-miRNAs contribute to the cardiotoxic responses induced by CKD-EVs.

Cardiotoxic CKD-miRNAs Impaired Contractile and Calcium-Handling Gene Expression

For a mechanistic understanding of our findings, we sought to uncover gene expression changes in CMs induced by novel cardiotoxic miRNAs uniquely enriched in CKD-EVs. We transfected the hiPSC-CMs with mimics of 3 miRNAs associated with contractile dysfunction (miR-2110, miR-320b, and miR-484) or a scramble control for 48 hours, followed by RNA sequencing (Figure 6A). This analysis revealed suppression of several contractile and calcium-handling genes (Figure 6B; Figures S23 and S24). Gene Set Enrichment Analysis of Gene Ontology Biological Process pathways revealed that contractile function, calcium handling, and metabolic processes were among the top 5 significantly suppressed pathways based on differentially expressed genes (eg, negative regulation of calcium channel activity, suppressed by miR-2110; myofibril assembly, suppressed by miR-320b; and mitochondrial ATP synthesis, suppressed by miR-484; Figure 6C through 6E), which correlated with the function of the miRNAs. Moreover, qRT-PCR analysis in hiPSC-CMs chronically treated (3 times, once every 3 days) with miR-2110, miR-320b, or miR-484 mimics showed downregulation of several calcium handling and contractile function associated genes, such as phospholamban (*PLN*) (miR-2110, miR-484), myosin-6 alpha heavy chain (*MYH6*) (miR-320b, miR-484) and Krüppel-like factors (*KLF*) (miR-2110; Figure 6F). Likewise, expression of *PLN* and ATPase Sarcoplasmic/Endoplasmic Reticulum Ca²⁺ Transporting 2 (*Atp2a2*) was found to be downregulated in the hearts of the CKD mice (Figure S25), suggesting that cardiotoxic miRNAs affect cardiac function by altering the expression of genes crucial for Ca²⁺ cycling and muscle contraction. Together, these data indicate numerous CKD-miRNAs synergistically limit CM and cardiac contractility.

miRNAs Associated With Circulating CKD-EVs Originate in the Kidney

To assess the role of CKD-plasma EVs in reno-cardiac crosstalk, we sought to determine whether circulating EV-miRNAs originate from the kidney. First, we tested whether mCKD-circulating and kidney-derived EVs harbor the same miRNAs signatures as hCKD-EVs (Figure 7A and 7B). Of the 9 key miRNAs detected in hCKD-EVs, 7 are evolutionarily conserved across mammals (Figure S26). qRT-PCR analysis revealed that 4 of those miRNAs (miR-130b-3p, 22-5p, 320-3p, and 423-5p) were significantly

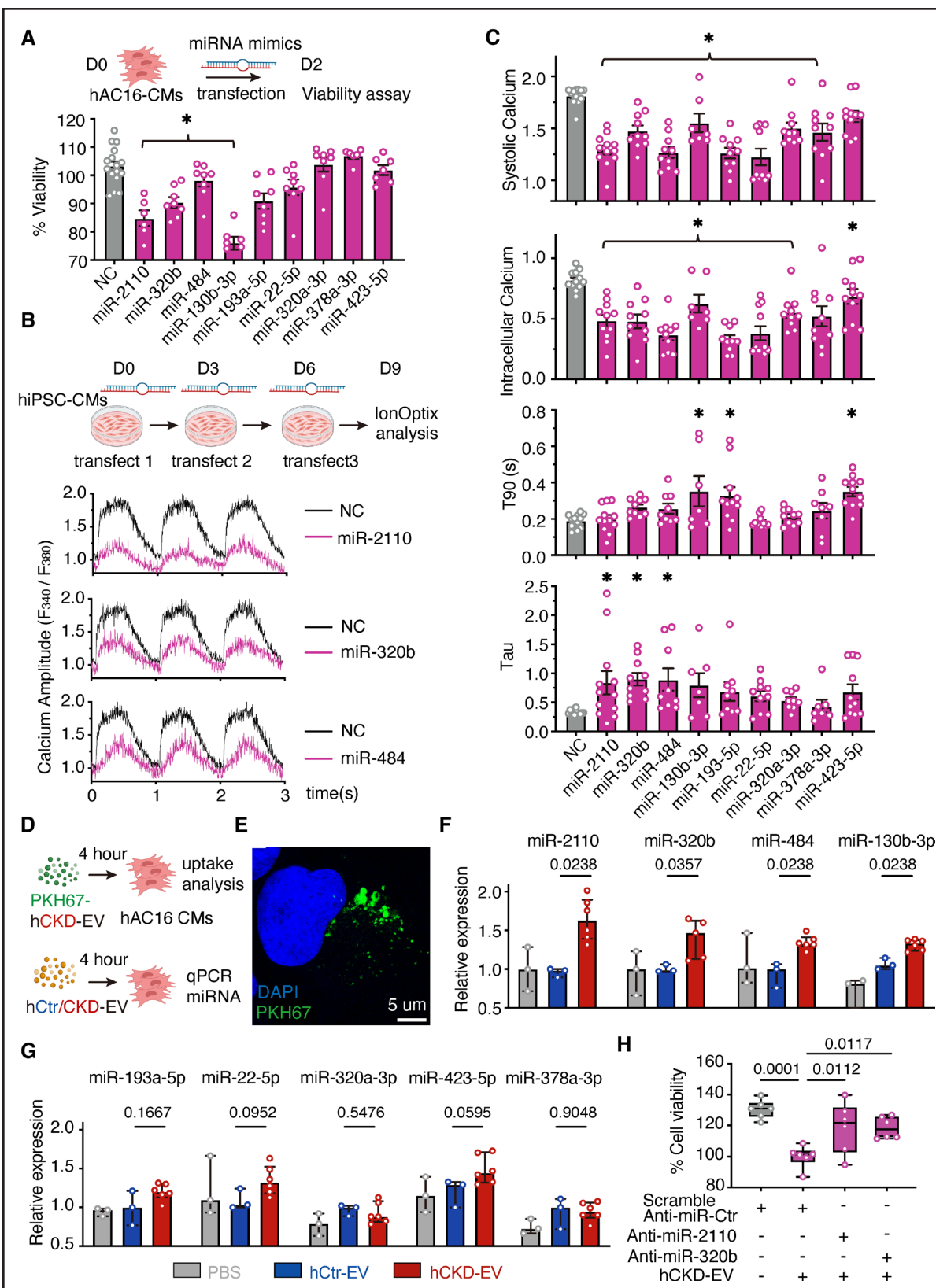


Figure 5. miRNAs enriched in hCKD-EVs contribute to their cardiotoxicity.

A, Viability of hAC16-CMs transfected with 9 selected miRNA mimics and one negative control ($n=6-16$). **B**, Schematic of calcium handling analysis in hiPSC-CMs treated with miRNA mimics. hiPSC-CMs were transfected with miRNA mimics every 3 days for a total of 3 times. Representative calcium amplitude transients through contraction-relaxation cycles of hiPSC-CMs treated with miR-2110, miR-320b, and miR-484 mimics as measured by IonOptix analysis. **C**, Quantification of calcium transients and contractility of hiPSC-CMs transfected (Continued)

Figure 5 Continued. with the same 9 miRNA mimics and one negative control ($n=12$). Quantification of systolic Ca^{2+} (F_{340}/F_{380}), intracellular Ca^{2+} (F_{340}/F_{380}), time constant for calcium decay (τ), and time for the Ca^{2+} signal (F_{340}/F_{380}) to rise from 10% to 90% (T90) (s). **D**, Schematic of study design evaluating uptake and gene regulation of hCKD-EVs. **E**, Confocal microscopy of PKH67-labeled hCKD-EV uptake in hAC16-CMs at 4 hours. **F** and **G**, qRT-PCR analysis of miRNA expressions in hAC16-CMs treated with equal counts of hCKD/Ctr-EVs (2e5 particles/cell; $n=3-6$). **H**, Viability of hAC16-CMs treated with hCKD-EVs and anti-miRNA, as indicated. hAC16-CMs were transfected with anti-miRNA (scramble control, miR-2110, or miR-320b) and then treated with hCKD-EVs after 6 hours. Cell viability MTT assay was performed 24 hours after treatment. Data in **A** through **C** are presented as mean \pm SEM. Data in **H** are presented as box-and-whisker plots. Data in **A** through **C** and **H** were analyzed with 1-way ANOVA with Dunnett multiple comparison test. * $P<0.05$. Data in **F** and **G** are presented as median with interquartile range and were analyzed with Mann-Whitney *U* test. CKD indicates chronic kidney disease; Ctr, control; hCKD-EV, plasma extracellular vesicles from patients with CKD; hCtr-EV, plasma extracellular vesicles from healthy control; hiPSC-CMs, human-induced pluripotent stem cell-derived cardiomyocytes; miR/miRNA, microRNA; NC, negative control; and PBS, phosphate-buffered saline.

upregulated in both circulating and kidney mCKD-EVs compared with mCtr-EVs (Figure 7A and 7B); miR-484 showed a similar trend but did not reach significance. miR-378a-3p had higher expression in plasma CKD-EVs but not in kidney CKD-EVs compared with controls, whereas miR-193-5p levels were unchanged. These data suggest both shared and distinct circulating miRNA cargo between mouse and human CKD-EVs. Further, these findings indicate the circulating CKD-miRNAs can originate renally.

Next, we investigated the kidney as a potential source of circulating CKD-EV-miRNAs. Transcription of pri-miRNAs, which give rise to mature miRNAs, is cell type- and tissue-specific²⁶ and their abundance in cells and tissues can predict the origin of circulating EV-miRNAs. To determine the origin of circulating mCKD-EV-miRNAs, we quantified the expression of their corresponding endogenous pri-miRNAs²⁷ in different tissues, including the kidney, heart, liver, blood (PBMCs), lungs, spleen, and skeletal muscle, from CKD and control mice, by qRT-PCR (Figure 7C; Figure S27). It is interesting that pri-miRNAs corresponding to 4 miRNAs (miR-320, -130, -484 and -22) (pri-miRNA [pri-miR]-320 correspond to miR-320-3p in mice because mice lack miR-320b) that were significantly upregulated in mCKD kidney and mCKD plasma EVs had significantly higher expression in mCKD kidneys than in mCtr kidneys (Figure 7D). It is important to note that these pri-miRNAs did not increase in mCKD heart, liver, lungs, spleen, PBMCs, or skeletal muscle (Figure 7D; Figure S27; except for pri-miR-22 in mCKD-PBMCs). These data show that the circulating cardiotoxic CKD-EV miRNAs have a predominantly renal origin, with PBMCs serving as an additional source.

To extend these findings to human data and to underpin their translational value, we performed a tissue deconvolution analysis²⁸ to determine whether the hCKD-EV miRNAs are unique to the diseased kidney. We estimated the relative tissue enrichment of all differentially expressed hCKD-EV-miRNAs and compared them to the publicly available, curated, tissue-specific, bulk-tissue miRNA expression profiles from the Genotype-Tissue Expression database²⁹ as a reference. Our deconvolution analysis found significantly higher hCKD-EV-miRNA relative enrichment in kidney cortex compared with its relative enrichment in control. These data indicate that kidney cortex, a major site of CKD

pathology, contributes significantly to circulating EV-miRNAs in patients with CKD, rather than liver, heart, lung, or other organs (Figure S28).

To identify the specific cell types contributing to CKD-EV-miRNAs, we prepared single-cell suspensions from the control and CKD kidneys and separated them into CD45^{+ve} immune cells, CD31^{+ve} endothelial cells, and the remaining CD31^{-ve}CD45^{-ve} renal cells (the latter group includes renal glomerular and tubular cells, podocytes, and fibroblasts; Figure 8A through 8D). We then examined CKD-pri-miRNA expressions in those cell groups. Four CKD-pri-miRNAs (pri-miR-130, -22, -320, and -484; Figure 7D) increased in renal tissue had significantly higher expression in CD31^{-ve}CD45^{-ve} renal cells (Figure 8E). Two CKD-pri-miRNAs (pri-miR-130b and -484) exhibited significantly higher expression in CD31^{+ve} endothelial cells (Figure 8E). It is interesting that none of the CKD-pri-miRNAs were enriched in CD45^{+ve} immune cells. These data indicated that CKD-EV-miRNAs within the CKD kidney have heterogeneous origins. It is remarkable that although CD45^{+ve} leukocytes numbers are markedly elevated in the CKD kidney (Figure 8B; Figure S29), they are not a substantial source of CKD pri-miRNAs or CKD-EV-miRNAs. This is the first direct evidence that circulating CKD-EV-miRNAs have renal origins.

DISCUSSION

Our study reports several new findings. First, we present the evidence that circulating EVs from patients with CKD, but not the EV-depleted fraction thereof, are cardiotoxic. CKD-EVs induce apoptosis, impair contractile function, and restrict Ca^{2+} handling in treated CMs. Second, we show that depleting circulating EVs in CKD mice recover cardiac function and ameliorate HF, even in the presence of CKD comorbidities. Third, we demonstrate that CKD-EVs are enriched in cardiotoxic miRNAs that originate from kidney cells. Taken together, these results outline a novel mechanism through which, during CKD, renal cells secrete CKD-EVs carrying cardiotoxic miRNAs to the circulation, thereby altering cardiac contractile gene expression and, with chronic exposure, causing HF (Figure 8F). Circulating CKD-EVs thus play a causal role in the pathogenesis of HF through a reno-cardiac communication axis.

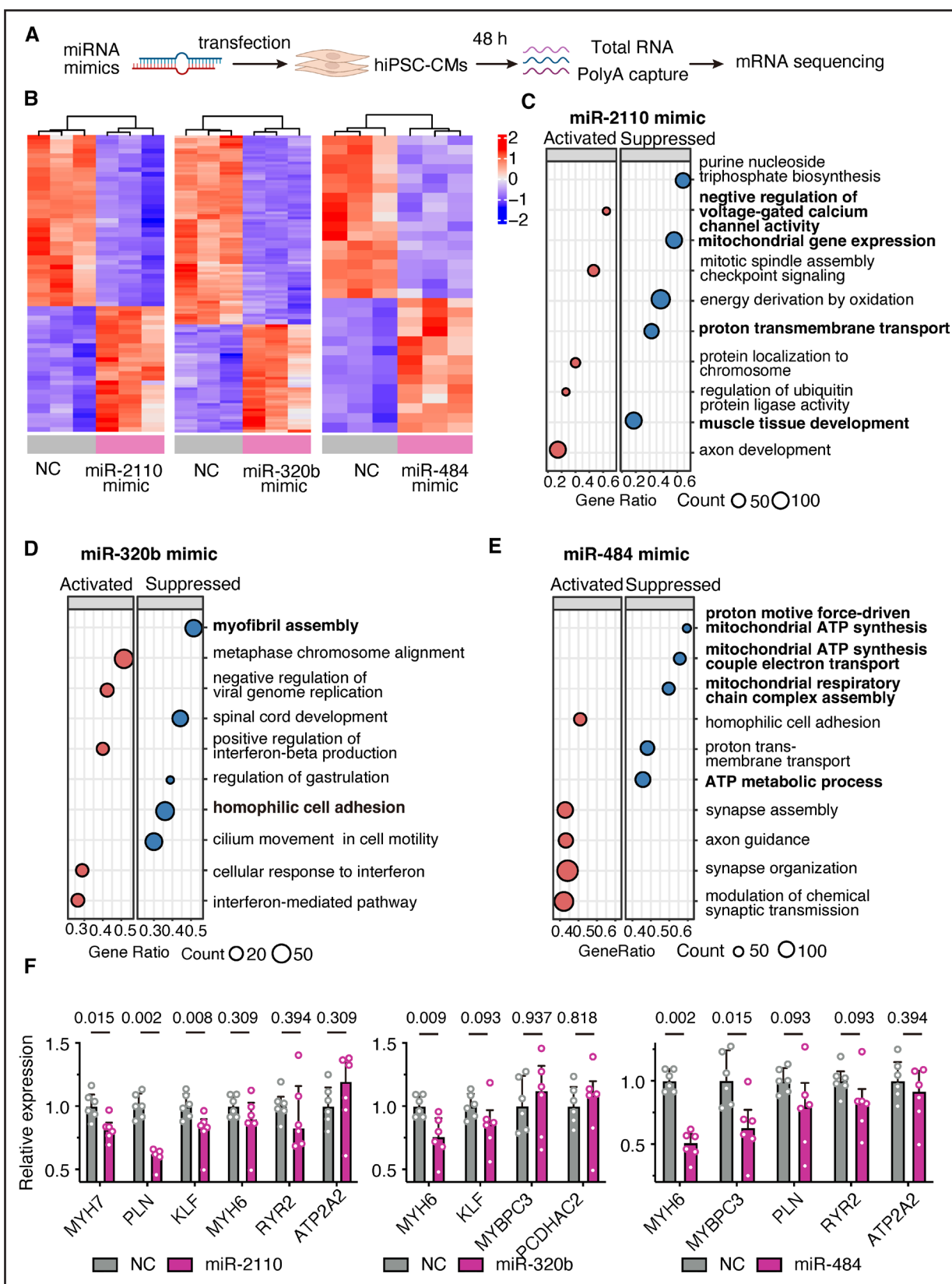


Figure 6. miRNAs enriched in hCKD-EVs impaired the contractility and calcium handling gene expression in human iPSC-derived cardiomyocytes.

A, Schematic of study design for mRNA sequencing of hiPSC-CMs transfected with miRNA mimics. **B**, Heatmap showing expression of differentially expressed genes in hiPSC-CMs transfected with miRNA mimics (miR-negative control [NC], miR-2110, miR-320b, and miR-484); the top 50 significantly differential expressed genes are listed in Tables S5 to S7. **C**, Gene Set Enrichment Analysis (GSEA) of (Continued)

Figure 6 Continued. gene ontology (GO) Biological Process pathways in hiPSC-CMs transfected with miR-2110, miR-320b (**D**), and miR-484 (**E**). The plot displays significantly enriched pathways grouped by activation or suppression. Dot size represents the number of genes involved (count), and the x axis shows the gene ratio. **F**, Expression of the calcium handling and contractile function-associated genes was assessed by qRT-PCR in hiPSC-CMs treated with miR-2110, miR-320b, or miR-484 mimics every 3 days for a total of 3 doses (n=6). Data in **F** are presented as median with interquartile range and were analyzed with Mann-Whitney *U* test. hiPSC-CMs indicates human-induced pluripotent stem cell-derived cardiomyocytes; and miR/miRNA, microRNA.

CKD and HF have a complex and interdependent relationship. Independently of comorbidities and other traditional and nontraditional CVD risk factors in patients with CKD, kidney dysfunction triggers the release of bioactive components that contribute to cardiac damage.³ In >70 studies of nondialyzed subjects with CKD, correcting for classical cardiovascular risk factors, such as hypertension, diabetes, and dyslipidemia, did not neutralize the impact of CKD on cardiovascular risk.^{3,30,31} That these traditional risk factors only partially explain the excess risk of CVD in patients with CKD points to additional kidney-derived molecular factors affecting cardiac function. However, no kidney- or plasma-derived risk factor that triggers HF at either a cellular or molecular level in patients with CKD has yet been identified, primarily because there is little systematic investigation in patients with reno-cardiac disease. Our study is the first to address this critical knowledge gap by exploring the direct cardiotoxic effects of CKD-associated molecular factors on CM and cardiac contractile functions.

EVs are an important component of circulating plasma. Most previous EV studies involving the reno-cardiac axis are observational or correlational in nature. For example, a CKD mouse study that reported proarrhythmic remodeling of the heart did not study reno-cardiac crosstalk.²¹ Another acute kidney injury murine study reported interleukin-33 signaling from kidney to heart³² but did not investigate the EVs. CKD-EVs from mice¹¹ and patients³³ have been shown to exacerbate vascular calcification, to limit angiogenesis,¹² and to serve as a surrogate marker of endothelial dysfunction in patients with end-stage renal disease.^{34–36} Collectively, these previous studies implicate circulating factors or EVs as contributors to CKD-induced HF but do not explicate the direct role CKD-EVs play in cardiotoxicity, contractility, and HF pathogenesis. In addition, none of these studies investigated reno-cardiac interactions or renal cell contributions to altered circulating EV cargo in CKD.

To bridge these knowledge gaps, we recruited patients with CKD and healthy control subjects, used a mouse model of modified adenine diet–induced CKD with HF, and used hiPSC-CMs to study the causal roles and mechanisms of CKD-EVs. We fully characterized hCKD-EVs and demonstrate that they are cardiotoxic and carry several proapoptotic and anticontractile miRNAs, including the human specific miRs 2110 and 320b. In addition, several hCKD-miRs are known to be associated with renal inflammation and fibrosis (miR-193a-5p³⁷), apoptosis (miR-130b-3p,^{38,39} miR-320-3p,^{40,41} miR-378a-3p⁴²), oxidative stress (miR-423-5p^{43,44}), and cardiac function (miR-320-3p^{41,45}). Overall,

our findings confirm that patients with CKD have significantly altered circulating CKD-EV and -EV-miR compositions. Cardiotoxic effects and miRNA signatures of human and mouse CKD-plasma-EVs were largely comparable. In addition, we demonstrated that pharmacologically depleting CKD-EVs by using GW ameliorated HF in CKD mice, even in the presence of other comorbidities, thus providing direct proof-of-concept evidence for the causal role of EVs in HF. Although GW reduced EV secretion from CKD kidneys (possibly through its effect on preventing intraluminal vesicle formation), it can impact lipid metabolism and inflammation.²⁵ These and other side effects of GW may have partially contributed to improved cardiac contractility in our CKD mouse model. Future studies with endogenous labeling of kidney EVs may reveal in-depth EV-based mechanisms in more detail.

Kidney-enriched miRNAs, which can be packaged into EVs and transported into circulation, mediate organ crosstalk.^{7,46} A proteomic analysis of cardiac EVs showed that some proteins in these EVs may originate from the kidney.⁴⁷ To date, few direct experimental methods can define the tissue or cellular origin of circulating EV miRNA cargo. Pri-miRNAs are precursors to mature miRNAs and are not typically found in circulating EVs.²⁷ Although pri-miRNAs are not a primary marker of EV origin, the tissue and cellular presence of pri-miRNAs can be used to infer the origins of circulating EV-miRNAs. It is interesting that high expression of many CKD plasma EV-miRNAs correlated with CKD kidney EV-miRNAs and their corresponding endogenous pri-miRNAs from the CKD kidneys, but not with pri-miRNAs from other organs such as the CKD heart, liver, lungs, spleen, or PBMCs from the blood (Figure 7D; Figure S27). Moreover, CD31^{-ve}CD45^{-ve} renal cells including renal tubular epithelial cells, podocytes, and fibroblasts, but not CD45^{+ve} immune or CD31^{+ve} endothelial cells, exhibited concomitantly increased CKD-EV-miRNA levels, which suggest these cells could be an origin of cardiotoxic miRNA-carrying EVs. We thus provided cumulative evidence of renal origin of CKD-EV-miRNAs using pri-miRNA expression from organs and sorted kidney cells from mice and in silico deconvolution data from humans. This is the first direct evidence that during CKD, altered circulating CKD-EV-miRNAs originate from kidney cells. Unequivocally demonstrating that kidney-derived EVs directly transfer to the heart through circulation would require elaborate kidney cell-specific genetic mouse models with endogenously labeled fluorescent EV markers; this may be a future line of inquiry.

It is remarkable that in our study, CKD-EV-miRNA expressions did not significantly differ between our

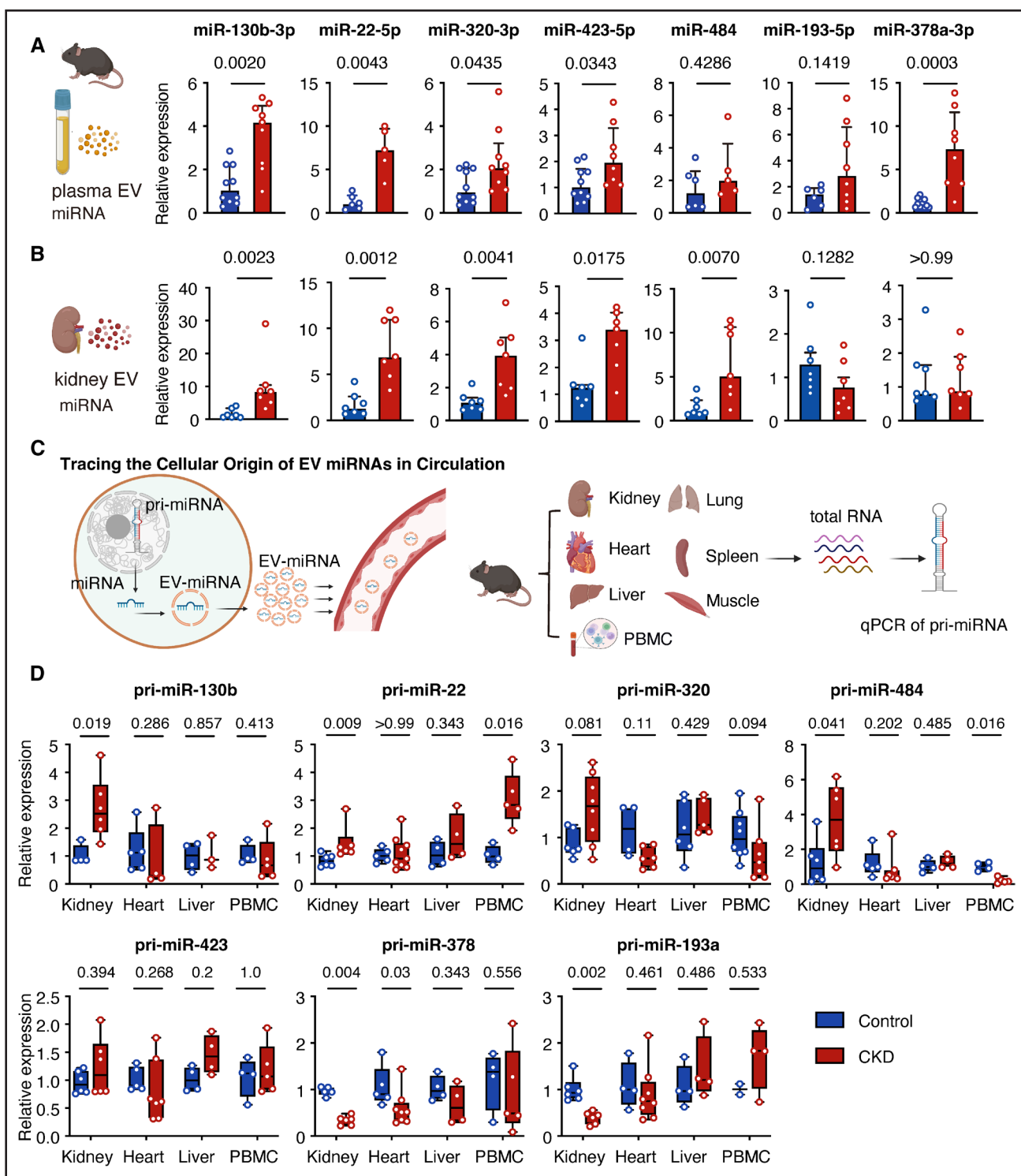


Figure 7. CKD-EV-miRNAs originate renally in CKD mice.

A, qRT-PCR analysis of miRNA expressions in mCKD-pEVs compared with mCtr-pEVs ($n=5-10$). **B**, qRT-PCR analysis of miRNA expression in mCKD-kEVs compared with mCtr-kEVs ($n=7$). **C**, Schematic of study design tracing the cellular origin of EV-miRNAs in circulation: expression of corresponding primary miRNA (pri-miRNA) was used to predict the cellular origin of mature EV-miRNAs. **D**, Expression of corresponding pri-miRNA transcripts in kidney, heart, liver, and PBMCs was assessed by qRT-PCR in CKD vs control mice ($n=3-8$). Data in **A** and **B** are presented as median with interquartile range and were analyzed with Mann-Whitney *U* test. Data in **D** are presented as box-and-whisker plots and were analyzed with Mann-Whitney *U* test with multiple comparisons; *P* values are unadjusted. CKD indicates chronic kidney disease; EVs, extracellular vesicles; miR/miRNA, microRNA; PBMC, peripheral blood mononuclear cells; and pri-miR, primary miRNA.

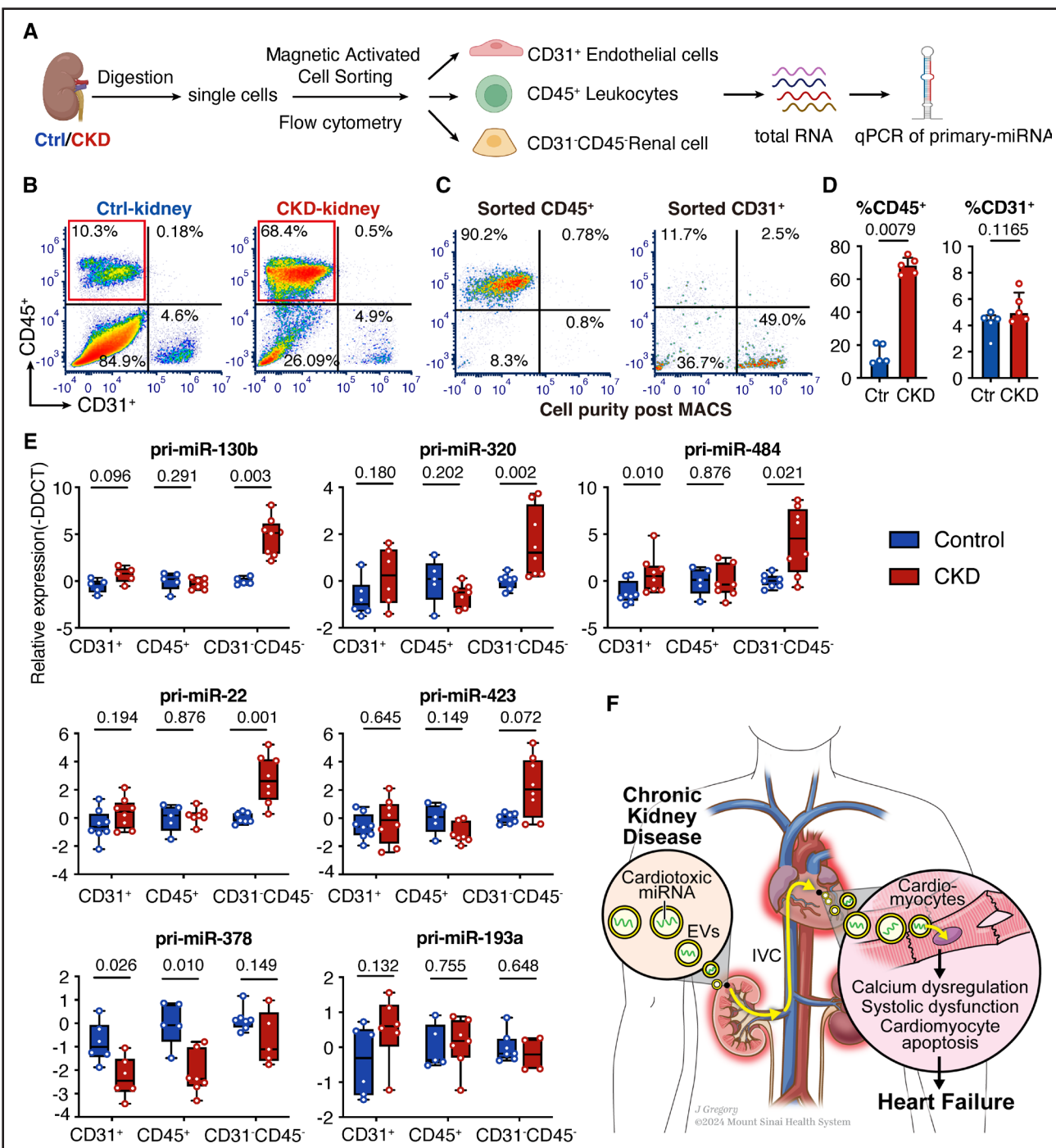


Figure 8. CKD-EV-miRNAs may have heterogeneous cellular origins in CKD kidneys.

A, Schematic of study plan to detect the origins of CKD-EV-miRNAs (through expression of their corresponding pri-miRNAs) from different cell types in the kidney. **B**, Representative flow cytometry analysis of CD45^{+ve} and CD31^{+ve} cells isolated from CKD kidneys compared with Ctr kidneys. **C**, Purity of CD45^{+ve} and CD31^{+ve} cell population was assessed by flow cytometry after magnetic-activated cell sorting (MACS). **D**, Quantification of %CD45^{+ve} cells and %CD31^{+ve} cells in CKD kidneys compared with Ctr kidneys ($n=5$). **E**, Expression of the corresponding pri-miRNA transcripts of selected CKD-EV-miRNAs in CD45^{+ve} leukocytes, CD31^{+ve} endothelial cells, and double-negative CD45^{-ve}CD31^{-ve} renal cells was assessed by qRT-PCR in CKD vs Ctr kidneys. **F**, Schematic illustrating the proposed mechanism by which EV-associated miRNAs secreted from CKD kidneys enter the circulation and contribute to heart failure development. Data in **D** are presented as median with interquartile range and were analyzed with Mann-Whitney *U* test. Data in **E** are presented as box-and-whisker plots and were analyzed with Mann-Whitney *U* test with multiple comparisons; *P* values are unadjusted. CKD indicates chronic kidney disease; Ctr, control; EVs, extracellular vesicles; IVC, inferior vena cava; MACS, magnetic-activated cell sorting; miR/miRNA, microRNA; and pri-miR, primary miRNA.

CKD(-)HF and CKD(+)HF cohorts, possibly because of heterogeneity within the CKD(-)HF group (percent ejection fraction >50). In concurrence, many CKD-EV-miRNA expressions correlated with traditional myocardial injury and mortality markers, such as hsTNI, NT-proBNP, and ANP, that suggest cardiac stress and subclinical cardiac damage in our CKD(-)HF cohort. These data are supported by previous observations that heart failure with preserved ejection fraction is more prevalent than heart failure with reduced ejection fraction in patients with CKD.⁴⁸ NT-proBNP, hsTnI, and ANP levels in CKD can be elevated because of both decreased renal clearance and increased production in response to cardiac stress.⁴⁹ Yet cutoffs for these prognostic markers, specifically in patients with heart failure with preserved ejection fraction and CKD, are still under active investigation.⁴⁹ Although elevated levels of these markers are valuable in assessing subclinical cardiac damage in CKD, they are not standalone diagnostics. Accurate diagnosis in this context requires integration with additional clinical assessments, such as echocardiography, cardiac magnetic resonance imaging, LV filling pressures, exercise capacity (6-minute walk test or peak oxygen consumption), symptoms (eg, New York Heart Association functional class evaluation), quality of life, and other objective measures. This underscores the potential of CKD-miRNAs in diagnosing HF early in patients with CKD even before the symptoms are clinically apparent, identifying individuals at higher risk of developing HF, or predicting disease severity and risk stratification of CKD-induced HF. That CKD-EV-miRNAs correlate with markers of myocardial injury and cluster in similar patterns between CKD±HF patients (*Figures S16 through S18*) could be attributed to their decreased renal clearance in CKD (low estimated glomerular filtration rate). Yet we have identified several EV-miRNAs with both increased and decreased expression in patients with CKD (Figure 4G; *Figure S12*), suggesting other factors, including increased production, uremic toxicity, or inflammation, or interplay between these factors, may contribute to their dysregulation. Higher levels of primary miRNAs in CKD kidneys in our study (Figure 7D) also confirmed increased miRNA biogenesis. To address the clearance mechanisms and the CKD specificity of the EV-miRNAs, future studies should systemically correlate CKD-EV-miRNA expressions with established HF markers in longitudinal comparisons of patients with CKD with and without HF, patients with CKD with heart failure with preserved ejection fraction, and patients with HF who do not have CKD. Moreover, patients with HF before and after a kidney transplant for end-stage renal disease can provide an ideal human model to investigate the functional relevance of EVs. Such hybrid clinical and basic science work can also map the complex relationship between HF and CKD and define the different disease phenotypes of the reno-cardiac axis.

Going forward, investigations expanding on our findings may address several important questions. Although

our functional and miRNA expression data provided valuable insights, our significantly younger control group may have introduced age-related bias. In addition, many of our controls were healthy according to their medical history, and clinical metadata were not uniformly available. On the other hand, all patients in our CKD cohort were clinically stable, received guideline-directed medical therapy, and had higher medication use that reflected the intensified therapeutic regimen necessitated by their disease state. Thirty percent of the patients with CKD in our functional contractility study (Figure 1L and 1M) received Ca²⁺ channel inhibitors, and 50% received beta-blockers. It is unlikely that these medications were transferred from plasma through isolated CKD-EVs (which were thoroughly washed and processed) in quantities that could significantly impact their cardiotoxic function. The cardiotoxic and anticontractile function of plasma and kidney EVs from CKD mice also confirmed the pathological role CKD-EVs play in HF, independent of the variations arising from comorbidities, age differences, or concomitant medications in human samples. Future studies to identify HF biomarkers in patients with CKD may need to recruit larger study populations with age-matched cohorts and use regression analysis for adjusted data sets.

EVs contain diverse cargo encompassing other RNA species, proteins, and lipids that reflect the pathophysiology of their originating cell. To comprehensively uncover the cardiotoxic factors in CKD-EVs, the identities and functions of those biomolecules must be investigated. CKD is a systemic disease with broad adverse effects, including on the endocrine and immune systems.⁵⁰ The molecular identities of EVs produced by various cell types need to be determined to comprehensively characterize pathogenic factors, including the systemic effect of uremic toxins on the biogenesis of EVs, contributing to HF in CKD. Moreover, although our study evaluated the cardiotoxic effects of circulating and kidney CKD-EV-miRNAs on CMs, to fully understand the molecular mechanisms underlying renal-cardiac crosstalk requires clarity about how EVs influence non-CMs, including immune cells, endothelial cells, and cardiac fibroblasts, within the heart.

Collectively, using human, mouse, and cell culture models, the work we report here demonstrated that CKD-EVs, through their renal-derived miRNA cargo, are key contributors to humoral cardiotoxicity in patients with CKD. Our study revealed CKD-EV-mediated molecular crosstalk between the kidney and the heart that plays a causal role in the pathogenesis of HF in CKD. Future studies on the cardiotoxic cargo of CKD-EVs could identify robust biomarkers for early HF diagnosis, prognosis, and monitoring as well as new therapeutic targets to treat chronic reno-cardiac disease.

ARTICLE INFORMATION

Received May 30, 2025; accepted October 10, 2025.

Affiliations

Cardiovascular Research Institute (X.L., N.R., A.G., S.Z., S.L.S., S.Y., A.P., A.S., S.S.), Department of Medicine, Cardiology (C.G.S.-G.), Department of Genetics and Genomic Sciences (D.S.), Department of Medicine, Division of Endocrinology, Diabetes and Bone Disease (C.J.L.), Pathology, Molecular and Cell-Based Medicine (N.C.D.), Mindich Child Health and Development Institute (N.C.D.), Department of Cell, Developmental and Regenerative Biology (N.C.D.), Icahn School of Medicine at Mount Sinai, New York, NY. Division of Nephrology, University of Virginia, Charlottesville (H.Y., M.H., U.E.). Department of Translational Research & Cellular Therapeutics, City of Hope, Los Angeles, CA (R.V.).

Acknowledgments

The authors acknowledge contributions from Dr Igor A. Shumilin at the University of Virginia for his help with institutional review board processing; Ms Zeynep S. Cakmak at the Icahn School of Medicine at Mount Sinai for maintaining hiPSC-CMs; Ms Jill Gregory at the Icahn School of Medicine at Mount Sinai for the illustration in Figure 8F; and Dr Kaley Joyes at the Icahn School of Medicine at Mount Sinai for editing the article.

Sources of Funding

This work was supported by grants from the National Institutes of Health (HL140469, HL124187, and HL148786 to S.S.; R01DK125856 and 1-INO-2025-1704-A-N to S.S. and R.V.; R21AG07848 to N.C.D. and S.S.; and R01DK133598 to U.E. and S.S.).

Disclosures

None.

Supplemental Material

Expanded Supplemental Methods

Tables S1–S7

Figures S1–S30

References 51–73

Minimum Information About a High-Throughput Sequencing Experiment (MIN-SEQE) Checklist

Strengthening the Reporting of Observational Studies in Epidemiology (STROBE) Checklist

Animal Research: Reporting of In Vivo Experiments (ARRIVE) Checklist

REFERENCES

- Francis A, Harhay MN, Ong ACM, Tummala Palli SL, Ortiz A, Foggo AB, Fliser D, Roy-Chaudhury P, Fontana M, Nangaku M, et al; American Society of Nephrology. Chronic kidney disease and the global public health agenda: an international consensus. *Nat Rev Nephrol*. 2024;20:473–485. doi: 10.1038/s41581-024-00820-6
- Tomey MI, Winston JA. Cardiovascular pathophysiology in chronic kidney disease: opportunities to transition from disease to health. *Ann Glob Health*. 2014;80:69–76. doi: 10.1016/j.aghs.2013.12.007
- Jankowski J, Floege J, Fliser D, Bohm M, Marx N. Cardiovascular disease in chronic kidney disease: pathophysiological insights and therapeutic options. *Circulation*. 2021;143:1157–1172. doi: 10.1161/CIRCULATIONAHA.120.050686
- Warrens H, Banerjee D, Herzog CA. Cardiovascular complications of chronic kidney disease: an introduction. *Eur Cardiol*. 2022;17:e13. doi: 10.1542/ecr.2021.54
- Liu M, Li XC, Lu L, Cao Y, Sun RR, Chen S, Zhang PY. Cardiovascular disease and its relationship with chronic kidney disease. *Eur Rev Med Pharmacol Sci*. 2014;18:2918–2926.
- Rogers MA, Aikawa E. MicroRNA extracellular vesicle stowaways in cell-cell communication and organ crosstalk. *Arterioscler Thromb Vasc Biol*. 2019;39:2448–2450. doi: 10.1161/ATVBAHA.119.313533
- Grange C, Bussolati B. Extracellular vesicles in kidney disease. *Nat Rev Nephrol*. 2022;18:499–513. doi: 10.1038/s41581-022-00586-9
- Kalluri R, McAndrews KM. The role of extracellular vesicles in cancer. *Cell*. 2023;186:1610–1626. doi: 10.1016/j.cell.2023.03.010
- Fu S, Zhang Y, Li Y, Luo L, Zhao Y, Yao Y. Extracellular vesicles in cardiovascular diseases. *Cell Death Discov*. 2020;6:68. doi: 10.1038/s41420-020-00305-y
- Raghav A, Singh M, Jeong GB, Giri R, Agarwal S, Kala S, Gautam KA. Extracellular vesicles in neurodegenerative diseases: a systematic review. *Front Mol Neurosci*. 2022;15:1061076. doi: 10.3389/fnmol.2022.1061076
- Koide T, Mandai S, Kitaoka R, Matsuki H, Chiga M, Yamamoto K, Yoshioka K, Yagi Y, Suzuki S, Fujiki T, et al. Circulating extracellular vesicle-propagated microRNA signature as a vascular calcification factor in chronic kidney disease. *Circ Res*. 2023;132:415–431. doi: 10.1161/CIRCRESAHA.122.321939
- Behrens F, Holle J, Chen CY, Ginsbach LF, Krause BC, Brunning U, Kriegel FL, Kaiser T, Szijarto IA, Anandakumar H, et al. Circulating extracellular vesicles as putative mediators of cardiovascular disease in paediatric chronic kidney disease. *J Extracell Vesicles*. 2025;14:e70062. doi: 10.1002/jev.270062
- Stevens PE, Ahmed SB, Carrero JJ, Foster B, Francis A, Hall RK, Herrington WG, Hill G, Inker LA, Kazancioğlu R, et al. KDIGO 2024 clinical practice guideline for the evaluation and management of chronic kidney disease. *Kidney Int*. 2024;105:S117–S314. doi: 10.1016/j.kint.2023.10.018
- Bettin B, Gasecka A, Li B, Dhondt B, Hendrix A, Nieuwland R, van der Pol E. Removal of platelets from blood plasma to improve the quality of extracellular vesicle research. *J Thromb Haemost*. 2022;20:2679–2685. doi: 10.1111/jth.15867
- Nanou A, Zeune LL, Terstappen L. Leukocyte-derived extracellular vesicles in blood with and without EpCAM enrichment. *Cells*. 2019;8:937. doi: 10.3390/cells8080937
- Ding M, Wang C, Lu X, Zhang C, Zhou Z, Chen X, Zhang C-Y, Zen K, Zhang C. Comparison of commercial exosome isolation kits for circulating exosomal microRNA profiling. *Anal Bioanal Chem*. 2018;410:3805–3814. doi: 10.1007/s00216-018-1052-4
- Takov K, Yellon DM, Davidson SM. Comparison of small extracellular vesicles isolated from plasma by ultracentrifugation or size-exclusion chromatography: yield, purity and functional potential. *J Extracell Vesicles*. 2019;8:1560809. doi: 10.1080/20013078.2018.1560809
- Faure V, Dou L, Sabatier F, Cerini C, Sampol J, Berland Y, Brunet P, Dignat-George F. Elevation of circulating endothelial microparticles in patients with chronic renal failure. *J Thromb Haemost*. 2006;4:566–573. doi: 10.1111/j.1538-7836.2005.01780.x
- Bueno P, Montes de Oca A, Madueno JA, Merino A, Martin-Malo A, Aljama P, Ramirez R, Rodriguez M, Carracedo J. Endothelial microparticles mediate inflammation-induced vascular calcification. *FASEB J*. 2015;29:173–181. doi: 10.1096/fj.14-249706
- Yang Q, Su S, Luo N, Cao G. Adenine-induced animal model of chronic kidney disease: current applications and future perspectives. *Ren Fail*. 2024;46:2336128. doi: 10.1080/0886022X.2024.2336128
- King BMN, Mintz S, Lin X, Morley GE, Schlamp F, Khodadadi-Jamayran A, Fishman GI. Chronic kidney disease induces proarrhythmic remodeling. *Circ Arrhythm Electrophysiol*. 2023;16:e011466. doi: 10.1161/CIRCEP.122.011466
- Crescitelli R, Lässer C, Lötvall J. Isolation and characterization of extracellular vesicle subpopulations from tissues. *Nat Protocols*. 2021;16:1548–1580. doi: 10.1038/s41596-020-00466-1
- Branco AF, Pereira SP, Gonzalez S, Gusev O, Rizvanov AA, Oliveira PJ. Gene expression profiling of H9c2 myoblast differentiation towards a cardiac-like phenotype. *PLoS One*. 2015;10:e0129303. doi: 10.1371/journal.pone.0129303
- AIrola MV, Shanbhogue P, Shamseddine AA, Guja KE, Senkal CE, Maini R, Bartke N, Wu BX, Obeid LM, Garcia-Diaz M, et al. Structure of human nSMase2 reveals an interdomain allosteric activation mechanism for ceramide generation. *Proc Natl Acad Sci U S A*. 2017;114:E5549–E5558. doi: 10.1073/pnas.1705134114
- Catalano M, O'Driscoll L. Inhibiting extracellular vesicles formation and release: a review of EV inhibitors. *J Extracell Vesicles*. 2020;9:1703244. doi: 10.1080/20013078.2019.1703244
- Moreau PR, Tomas Bosch V, Bouvy-Liivrand M, Öunap K, Örd T, Pulkkinen HH, Pöhlönen P, Heinäniemi M, Ylä-Hertuala S, Laakkonen JP, et al. Profiling of primary and mature miRNA expression in atherosclerosis-associated cell types. *Arterioscler Thromb Vasc Biol*. 2021;41:2149–2167. doi: 10.1161/ATVBAHA.121.315579
- O'Brien J, Hayder H, Zayed Y, Peng C. Overview of microRNA biogenesis, mechanisms of actions, and circulation. *Front Endocrinol (Lausanne)*. 2018;9:402. doi: 10.3389/fendo.2018.00402
- Zhu S, Yang H, Liu J, Fu Q, Huang W, Chen Q, Teschendorff AE, He Y, Yang Z. An improved reference library and method for accurate cell-type deconvolution of bulk-tissue miRNA data. *Nat Commun*. 2025;16:5508. doi: 10.1038/s41467-025-60521-x
- Lonsdale J, Thomas J, Salvatore M, Phillips R, Lo E, Shad S, Hasz R, Walters G, Garcia F, Young N, et al. The Genotype-Tissue Expression (GTEx) project. *Nat Genet*. 2013;45:580–585. doi: 10.1038/ng.2653
- Falconi CA, Junho C, Fogaca-Ruiz F, Vernier ICS, da Cunha RS, Stinghen AEM, Carneiro-Ramos MS. Uremic toxins: an alarming danger concerning

- the cardiovascular system. *Front Physiol.* 2021;12:686249. doi: 10.3389/fphys.2021.686249
31. Vanholder R, Argiles A, Baurmeister U, Brunet P, Clark W, Cohen G, De Deyn PP, Deppisch R, Descamps-Latscha B, Henle T, et al. Uremic toxicity: present state of the art. *Int J Artif Organs.* 2001;24:695–725. doi: 10.1177/039139880102401004
 32. Florens N, Kasam RK, Rudman-Melnick V, Lin SC, Prasad V, Molkentin JD. Interleukin-33 mediates cardiomyopathy after acute kidney injury by signaling to cardiomyocytes. *Circulation.* 2023;147:746–758. doi: 10.1161/CIRCULATIONAHA.122.063014
 33. Viegas CSB, Santos L, Macedo AL, Matos AA, Silva AP, Neves PL, Staes A, Gevaert K, Morais R, Vermeer C, et al. Chronic kidney disease circulating calciprotein particles and extracellular vesicles promote vascular calcification. *Arterioscler Thromb Vasc Biol.* 2018;38:575–587. doi: 10.1161/ATVBAHA.117.310578
 34. Roumeliotis S, Mallamaci F, Zoccali C. Endothelial dysfunction in chronic kidney disease, from biology to clinical outcomes: a 2020 update. *J Clin Med.* 2020;9:2359. doi: 10.3390/jcm9082359
 35. Lu GY, Xu RJ, Zhang SH, Qiao Q, Shen L, Li M, Xu DY, Wang ZY. Alteration of circulatory platelet microparticles and endothelial microparticles in patients with chronic kidney disease. *Int J Clin Exp Med.* 2015;8:16704–16708.
 36. Amabile N, Guerin AP, Leroyer A, Mallat Z, Nguyen C, Boddaert J, London GM, Tedgui A, Boulanger CM. Circulating endothelial microparticles are associated with vascular dysfunction in patients with end-stage renal failure. *J Am Soc Nephrol.* 2005;16:3381–3388. doi: 10.1681/ASN.2005050535
 37. Bharati J, Kumar M, Kumar N, Malhotra A, Singh PC. MicroRNA193a: an emerging mediator of glomerular diseases. *Biomolecules.* 2023;13:1743. doi: 10.3390/biom13121743
 38. Gan L, Xie D, Liu J, Bond Lau W, Christopher TA, Lopez B, Zhang L, Gao E, Koch W, Ma XL, et al. Small extracellular microvesicles mediated pathological communications between dysfunctional adipocytes and cardiomyocytes as a novel mechanism exacerbating ischemia/reperfusion injury in diabetic mice. *Circulation.* 2020;141:968–983. doi: 10.1161/CIRCULATIONAHA.119.042640
 39. Qi Z, Liu R, Ju H, Huang M, Li Z, Li W, Wang Y. microRNA-130b-3p attenuates septic cardiomyopathy by regulating the AMPK/mTOR signaling pathways and directly targeting ACSL4 against ferroptosis. *Int J Biol Sci.* 2023;19:4223–4241. doi: 10.7150/ijbs.82287
 40. Tian ZQ, Jiang H, Lu ZB. MiR-320 regulates cardiomyocyte apoptosis induced by ischemia-reperfusion injury by targeting AKIP1. *Cell Mol Biol Lett.* 2018;23:41. doi: 10.1186/s11658-018-0105-1
 41. Ren XP, Wu J, Wang X, Sartor MA, Jones K, Qian J, Nicolaou P, Pritchard TJ, Fan GC. MicroRNA-320 is involved in the regulation of cardiac ischemia-reperfusion injury by targeting heat-shock protein 20. *Circulation.* 2009;119:2357–2366. doi: 10.1161/CIRCULATIONAHA.108.814145
 42. Tan J, Shen J, Zhu H, Gong Y, Zhu H, Li J, Lin S, Wu G, Sun T. miR-378a-3p inhibits ischemia/reperfusion-induced apoptosis in H9C2 cardiomyocytes by targeting TRIM55 via the DUSP1-JNK1/2 signaling pathway. *Aging (Albany NY).* 2020;12:8939–8952. doi: 10.18632/aging.103106
 43. Yuan XP, Liu LS, Chen CB, Zhou J, Zheng YT, Wang XP, Han M, Wang CX. MicroRNA-423-5p facilitates hypoxia/reoxygenation-induced apoptosis in renal proximal tubular epithelial cells by targeting GSTM1 via endoplasmic reticulum stress. *Oncotarget.* 2017;8:82064–82077. doi: 10.18632/oncotarget.18289
 44. Zhu X, Lu X. MiR-423-5p inhibition alleviates cardiomyocyte apoptosis and mitochondrial dysfunction caused by hypoxia/reoxygenation through activation of the wnt/beta-catenin signaling pathway via targeting MYBL2. *J Cell Physiol.* 2019;234:22034–22043. doi: 10.1002/jcp.28766
 45. Zhang X, Yuan S, Li H, Zhan J, Wang F, Fan J, Nie X, Wang Y, Wen Z, Chen Y, et al. The double face of miR-320: cardiomyocytes-derived miR-320 deteriorated while fibroblasts-derived miR-320 protected against heart failure induced by transverse aortic constriction. *Signal Transduct Target Ther.* 2021;6:69. doi: 10.1038/s41392-020-00445-8
 46. Mahtal N, Lenoir O, Tinel C, Anglicheau D, Tharaux P-L. MicroRNAs in kidney injury and disease. *Nat Rev Nephrol.* 2022;18:643–662. doi: 10.1038/s41581-022-00608-6
 47. Claridge B, Rai A, Fang H, Matsumoto A, Luo J, McMullen JR, Greening DW. Proteome characterisation of extracellular vesicles isolated from heart. *Proteomics.* 2021;21:2100026. doi: 10.1002/pmic.202100026
 48. Yu AS, Pak KJ, Zhou H, Shaw SF, Shi J, Broder BI, Sim JJ. All-cause and cardiovascular-related mortality in CKD patients with and without heart failure: a population-based cohort study in Kaiser Permanente Southern California. *Kidney Med.* 2023;5:100624. doi: 10.1016/j.xkme.2023.100624
 49. Kula A, Bansal N. Applications of cardiac biomarkers in chronic kidney disease. *Curr Opin Nephrol Hypertens.* 2022;31:534–540. doi: 10.1097/MNH.0000000000000829
 50. Tinti F, Lai S, Noce A, Rotondi S, Marrone G, Mazzaferro S, Di Daniele N, Mitterhofer AP. Chronic kidney disease as a systemic inflammatory syndrome: update on mechanisms involved and potential treatment. *Life (Basel).* 2021;11:419. doi: 10.3390/life11050419
 51. van der Velde M, Matsushita K, Coresh J, Astor BC, Woodward M, Levey A, de Jong PE, Gansevoort RT, van der Velde M, Matsushita K, et al; Chronic Kidney Disease Prognosis Consortium. Lower estimated glomerular filtration rate and higher albuminuria are associated with all-cause and cardiovascular mortality. A collaborative meta-analysis of high-risk population cohorts. *Kidney Int.* 2011;79:1341–1352. doi: 10.1038/ki.2010.536
 52. Matsushita K, van der Velde M, Astor BC, Woodward M, Levey AS, de Jong PE, Coresh J, Gansevoort RT; Chronic Kidney Disease Prognosis Consortium. Association of estimated glomerular filtration rate and albuminuria with all-cause and cardiovascular mortality in general population cohorts: a collaborative meta-analysis. *Lancet.* 2010;375:2073–2081. doi: 10.1016/S0140-6736(10)60674-5
 53. Gansevoort RT, Correa-Rotter R, Hemmelgarn BR, Jafar TH, Heerspink HJ, Mann JF, Matsushita K, Wen CP. Chronic kidney disease and cardiovascular risk: epidemiology, mechanisms, and prevention. *Lancet.* 2013;382:339–352. doi: 10.1016/S0140-6736(13)60595-4
 54. Heidenreich PA, Bozkurt B, Aguilar D, Allen LA, Byun JJ, Colvin MM, Deswal A, Drazner MH, Dunlay SM, Evers LR, et al; ACC/AHA Joint Committee Members. 2022 AHA/ACC/HFSA guideline for the management of heart failure: a report of the American College of Cardiology/American Heart Association Joint Committee on Clinical Practice Guidelines. *Circulation.* 2022;145:e895–e1032. doi: 10.1161/CIR.0000000000001063
 55. Wickramasinghe NM, Sachs D, Shewale B, Gonzalez DM, Dhanan-Krishnan P, Torre D, LaMarca E, Raimo S, Darioli R, Serasinghe MN, et al. PPARdelta activation induces metabolic and contractile maturation of human pluripotent stem cell-derived cardiomyocytes. *Cell Stem Cell.* 2022;29:559–576. e7. doi: 10.1016/j.stem.2022.02.011
 56. Angermann CE, Santos-Gallego CG, Requena-Ibanez JA, Sehner S, Zeller T, Gerhardt LMS, Maack C, Sanz J, Frantz S, Fuster V, et al. Empagliflozin effects on iron metabolism as a possible mechanism for improved clinical outcomes in non-diabetic patients with systolic heart failure. *Nat Cardiovasc Res.* 2023;2:1032–1043. doi: 10.1038/s44161-023-00352-5
 57. He H, Mulhern RM, Oldham WM, Xiao W, Lin YD, Liao R, Loscalzo J. L-2-hydroxyglutarate protects against cardiac injury via metabolic remodeling. *Circ Res.* 2022;131:562–579. doi: 10.1161/CIRCRESAHA.122.321227
 58. Santos-Gallego CG, Requena-Ibanez JA, San Antonio R, Garcia-Ropero A, Ishikawa K, Watanabe S, Picatoste B, Vargas-Delgado AP, Flores-Umanzor EJ, Sanz J, et al. Empagliflozin ameliorates diastolic dysfunction and left ventricular fibrosis/stiffness in nondiabetic heart failure: a multimodality study. *JACC Cardiovasc Imaging.* 2021;14:393–407. doi: 10.1016/j.jcmg.2020.07.042
 59. Swain L, Reyelt L, Bhave S, Qiao X, Thomas CJ, Zweck E, Crowley P, Boggins C, Esposito M, Chin M, et al. Transvalvular ventricular unloading before reperfusion in acute myocardial infarction. *J Am Coll Cardiol.* 2020;76:684–699. doi: 10.1016/j.jacc.2020.06.031
 60. Santos-Gallego CG, Requena-Ibanez JA, Picatoste B, Fardman B, Ishikawa K, Mazurek R, Pieper M, Sartori S, Rodriguez-Capitan J, Fuster V, et al. Cardioprotective effect of empagliflozin and circulating ketone bodies during acute myocardial infarction. *Circ Cardiovasc Imaging.* 2023;16:e015298. doi: 10.1161/CIRCIMAGING.123.015298
 61. Santos-Gallego CG, Requena-Ibanez JA, San Antonio R, Ishikawa K, Watanabe S, Picatoste B, Flores E, Garcia-Ropero A, Sanz J, Hajjar RJ, et al. Empagliflozin ameliorates adverse left ventricular remodeling in nondiabetic heart failure by enhancing myocardial energetics. *J Am Coll Cardiol.* 2019;73:1931–1944. doi: 10.1016/j.jacc.2019.01.056
 62. Ritchie ME, Phipson B, Wu D, Hu Y, Law CW, Shi W, Smyth GK. limma powers differential expression analyses for RNA-sequencing and microarray studies. *Nucleic Acids Res.* 2015;43:e47. doi: 10.1093/nar/gkv007
 63. Gu Z. Complex heatmap visualization. *Imeta.* 2022;1:e43. doi: 10.1002/im2.43
 64. Xiao F, Zuo Z, Cai G, Kang S, Gao X, Li T. miRecords: an integrated resource for microRNA-target interactions. *Nucleic Acids Res.* 2009;37:D105–D110. doi: 10.1093/nar/gkn851
 65. Hsu SD, Lin FM, Wu WY, Liang C, Huang WC, Chan WL, Tsai WT, Chen GZ, Lee CJ, Chiu CM, et al. miRTarBase: a database curates experimentally validated microRNA-target interactions. *Nucleic Acids Res.* 2011;39:D163–D169. doi: 10.1093/nar/gkq1107

66. Vergoulis T, Vlachos IS, Alexiou P, Georgakilas G, Maragakis M, Reczko M, Gerangelos S, Koziris N, Dalamagas T, Hatzigeorgiou AG. TarBase 6.0: capturing the exponential growth of miRNA targets with experimental support. *Nucleic Acids Res.* 2012;40:D222–D229. doi: 10.1093/nar/gkr1161
67. Ru Y, Kechris KJ, Tabakoff B, Hoffman P, Radcliffe RA, Bowler R, Mahaffey S, Rossi S, Calin GA, Bemis L, et al. The multiMiR R package and database: integration of microRNA-target interactions along with their disease and drug associations. *Nucleic Acids Res.* 2014;42:e133. doi: 10.1093/nar/gku631
68. Kanehisa M, Furumichi M, Sato Y, Kawashima M, Ishiguro-Watanabe M. KEGG for taxonomy-based analysis of pathways and genomes. *Nucleic Acids Res.* 2023;51:D587–D592. doi: 10.1093/nar/gkac963
69. Wu T, Hu E, Xu S, Chen M, Guo P, Dai Z, Feng T, Zhou L, Tang W, Zhan L, et al. clusterProfiler 4.0: A universal enrichment tool for interpreting omics data. *Innovation (Camb).* 2021;2:100141. doi: 10.1016/j.xinn.2021.100141
70. Ghanim H, Batra M, Green K, Hejna J, Abuaysheh S, Makdissi A, Chaudhuri A, Dandona P. Dapagliflozin reduces systolic blood pressure and modulates vasoactive factors. *Diabetes Obes Metab.* 2021;23:1614–1623. doi: 10.1111/dom.14377
71. Nougué H, Pezel T, Picard F, Sadoune M, Arrigo M, Beauvais F, Launay JM, Cohen-Solal A, Vodovar N, Logeart D. Effects of sacubitril/valsartan on neprilysin targets and the metabolism of natriuretic peptides in chronic heart failure: a mechanistic clinical study. *Eur J Heart Fail.* 2019;21:598–605. doi: 10.1002/ejhf.1342
72. Love MI, Huber W, Anders S. Moderated estimation of fold change and dispersion for RNA-seq data with DESeq2. *Genome Biol.* 2014;15:550. doi: 10.1186/s13059-014-0550-8
73. Yu G, Wang L-G, Han Y, He Q-Y. clusterProfiler: an R package for comparing biological themes among gene clusters. *OMICS J Integr Biol.* 2012;16:284–287. doi: 10.1089/omi.2011.0118